REPORT DOCUMENTATION PAGE

Form Approved
OMB No. 0704-0188

1. AGENCY USE ONLY (Leave blank)	2. REPORT DATE	3. REPORT TYPE AND DATES COVERED
		Final, 06/08/1998 - 09/30/1998

4. TITLE AND SUBTITLE
INVESIGATION OF CONTROL SYSTEM TECHNOLOGIES FOR PERFORMANCE IMPROVEMENT

5. FUNDING NUMBERS
Contract number:
DAAH01-91-D-R002 D.O. #127
Account: 5-20199
Award: $19,961

6. AUTHOR(S)
Yuri B. Shtessel

7. PERFORMING ORGANIZATION NAME(S) AND ADDRESS(ES)
University of Alabama in Huntsville
301 Sparkman Drive
Huntsville, AL 35899

8. PERFORMING ORGANIZATION REPORT NUMBER

9. SPONSORING/MONITORING AGENCY NAME(S) AND ADDRESS(ES)
US Army Aviation and Missile Command
AMSAM-AC-RD-BB
Attn: Ms. Belva Lynn
Redstone Arsenal, AL 35898-5280

10. SPONSORING/MONITORING AGENCY REPORT NUMBER

11. SUPPLEMENTARY NOTES

19981118 101

12a. DISTRIBUTION/AVAILABILITY STATEMENT

12b. DISTRIBUTION CODE

13. ABSTRACT *(Maximum 200 words)*

Engineering analysis has been performed to investigate the implementation of a sliding mode controller algorithm that will reduce sensitivity to feedback noise in Control Actuation Systems (CAS) such as those used on Guided MLRS, Low Cost Precision Kill (LCPK), and Compact Kinetic Energy Missile (CKEM). The GFE model of the CAS was used to demonstrate performance enhancement achieved with the sliding mode controller for a variety of potential noise sources. Two types of sliding mode controllers: a two-loop SMC and a single loop SMC have been designed, addressing the servomechanism output tracking problem. Both SMC's demonstrate high accuracy following of load position command profiles. Robustness to disturbances and noise voltage has been demonstrated as well. Both SMC's have been implemented in a relay format and a PWM format. The control voltage operates in a high frequency switching mode in both formats. It is recommended to use SMC's in a PWM format, which provides better protection against various noises.

14. SUBJECT TERMS

15. NUMBER OF PAGES
64

16. PRICE CODE

17. SECURITY CLASSIFICATION OF REPORT	18. SECURITY CLASSIFICATION OF THIS PAGE	19. SECURITY CLASSIFICATION OF ABSTRACT	20. LIMITATION OF ABSTRACT
Unclassified	Unclassified	Unclassified	

PLEASE CHECK THE APPROPRIATE BLOCK BELOW

DAO# _____

☐ _____ copies are being forwarded. Indicate whether Statement A, B, C, D, E, F, or X applies.

☒ DISTRIBUTION STATEMENT A:
APPROVED FOR PUBLIC RELEASE: DISTRIBUTION IS UNLIMITED

☐ DISTRIBUTION STATEMENT B:
DISTRIBUTION AUTHORIZED TO U.S. GOVERNMENT AGENCIES ONLY; (indicate Reason and Date). OTHER REQUESTS FOR THIS DOCUMENT SHALL BE REFERRED TO (Indicate Controlling DoD Office).

☐ DISTRIBUTION STATEMENT C:
DISTRIBUTION AUTHORIZED TO U.S. GOVERNMENT AGENCIES AND THEIR CONTRACTS (Indicate Reason and Date). OTHER REQUESTS FOR THIS DOCUMENT SHALL BE REFERRED TO (Indicate Controlling DoD Office).

☐ DISTRIBUTION STATEMENT D:
DISTRIBUTION AUTHORIZED TO DoD AND U.S. DoD CONTRACTORS ONLY; (Indicate Reason and Date). OTHER REQUESTS SHALL BE REFERRED TO (Indicate Controlling DoD Office).

☐ DISTRIBUTION STATEMENT E:
DISTRIBUTION AUTHORIZED TO DoD COMPONENTS ONLY; (Indicate Reason and Date). OTHER REQUESTS SHALL BE REFERRED TO (Indicate Controlling DoD Office).

☐ DISTRIBUTION STATEMENT F:
FUTHER DISSEMINATION ONLY AS DIRECTED BY (Indicate Controlling DoD Office and Date) or HIGHER DoD AUTHORITY.

☐ DISTRIBUTION STATEMENT X:
DISTRIBUTION AUTHORIZED TO U.S. GOVERNMENT AGENCIES AND PRIVATE INDIVIDUALS OR ENTERPRISES ELIGIBLE TO OBTAIN EXPORT-CONTROLLED TECHNICAL DATA IN ACCORDANCE WITH DoD DIRECTIVE 5230.25. WITHHOLDING OF UNCLASSIFIED TECHNICAL DATA FROM PUBLIC DISCLOSURE, 6 Nov 1984 (indicate date of determination). CONTROLLING DoD OFFICE IS (Indicate Controlling DoD Office).

☐ This document was previously forwarded to DTIC on _____ (date) and the AD number is _____.

☐ In accordance with provisions of DoD instructions. The document requested is not supplied because:

☐ It will be published at a later date. (Enter approximate date, if known).

☐ Other. (Give Reason)

DoD Directive 5230.24, "Distribution Statements on Technical Documents," 18 Mar 87, contains seven distribution statements, as described briefly above. Technical Documents must be assigned distribution statements.

Yuri Shtessel
Print or Type Name

Yuri Shtessel
Authorized Signature/Date

(256) 890-6164
Telephone Number

Technical Report

prepared for

U.S. Army Aviation & Missile Command, Redstone Arsenal, AL 35898

INVESIGATION OF

CONTROL SYSTEM TECHNOLOGIES

FOR PERFORMANCE IMPROVEMENT

Authors: **Dr. Yuri B. Shtessel, Principal Investigator**

Department of Electrical and Computer Engineering

University of Alabama in Huntsville, Huntsville, AL 35899

ph: (256)890-6164, fax: (256)890-6803, shtessel@ece.uah.edu

Contract Number: DAAH01-91-D-R002 D.O. #127

Period of Performance: 06/08/1998 - 09/30/1998

Final Report Due: 10/31/1998

Award: $19,961

1998

Table of Contents

1. Statement of Work

Engineering analysis must be performed to investigate the implementation of a sliding mode controller algorithm that will reduce sensitivity to feedback noise in Control Actuation Systems (CAS) such as those used on Guided MLRS, Low Cost Precision Kill (LCPK), and Compact Kinetic Energy Missile (CKEM). The GFE model of the CAS shall be used to demonstrate performance enhancement achieved with the sliding mode controller for a variety of potential noise sources.

2. Plant Description and Problem Formulation

The control problem, which is addressed in this technical report, consists of controlling a nonlinear servomechanism affected by noise. A block-diagram of the servomechanism with disturbance and noise are shown in figures 1 and 2

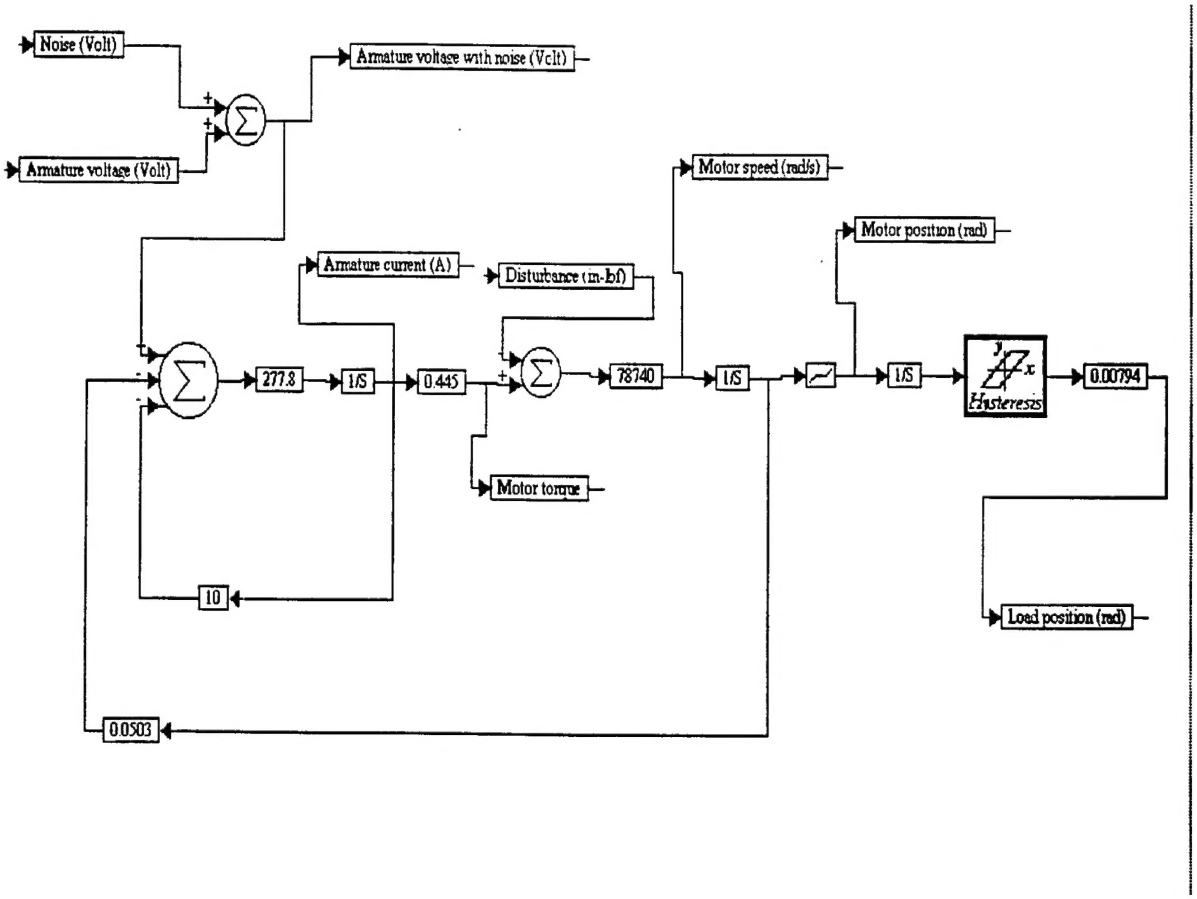

Fig. 1 A block-diagram of the servomechanism

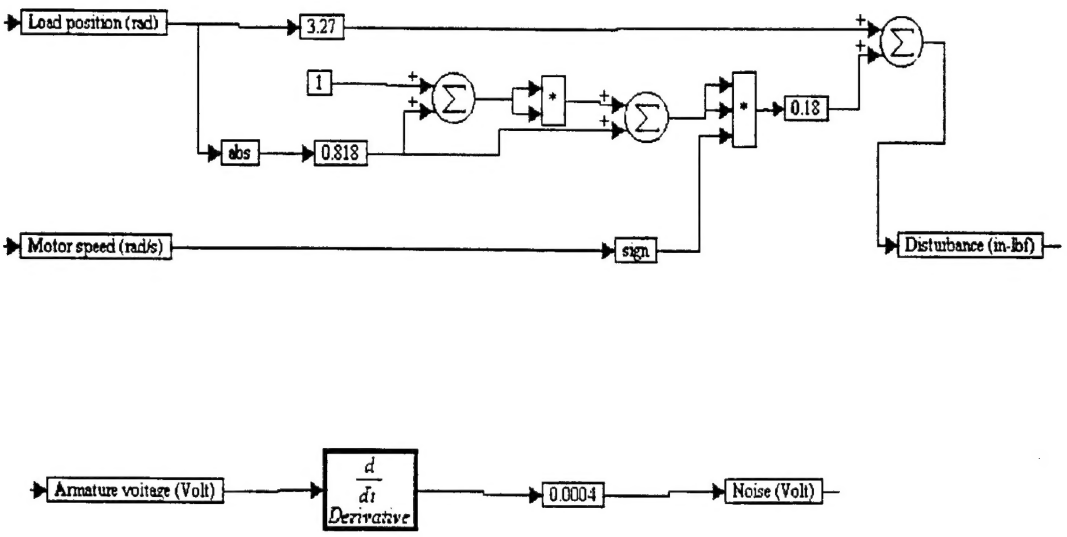

Fig. 2 A block-diagram of disturbance and noise

Neglecting backlash and hysteresis on the step of a sliding mode controller design the state variable model of the servomechanism (figures 1 and 2) is derived as follows:

$$\begin{cases} \dfrac{d\theta_L}{dt} = \dfrac{1}{n_g}\omega_m \\ \dfrac{d\omega_m}{dt} = \dfrac{1}{J}\left[k_t i_a - F(.)\right] \\ \dfrac{di_a}{dt} = \dfrac{1}{L_a}\left[v_a + n_v - R_a i_a - k_b \omega_m\right] \\ y = \theta_l \end{cases}, \qquad (1)$$

where

θ_L is position of the load *(rad)*, i_a is an armature current *(A)*, ω_m is motor angular velocity *(rad/s)*, $n_g = 125.9$ an actuator gear ratio, $\theta_m = n_g\theta_L$ is position of the motor (rad), $|v_a| \le 31$ is armature voltage *(V)*, n_v is voltage noise *(V)*, $k_t = 0.445$ is a torque constant $(in-lbf/A)$, k_b is back-EMF constant *(V/rad/s)*, $R_a = 10\Omega$ is motor winding resistance, $L_a = 0.0036H$ is motor winding inductance, $J_t = 0.0000125$ is total inertia reflected to the motor $(in-lbf-s^2)$, $J_L = 0.003$ is load inertia $(in-lbf-s^2)$, $J = J_t + \frac{J_L}{n_g^2} = 0.0000127$ is total inertia $(in-lbf-s^2)$, $F(.) = 3.27\theta_L + 0.18\,sign\theta_m\left[0.818|\theta_L| + (0.818|\theta_L|+1)^2\right]^2$ is disturbance torque $(in-lbf)$.

The servomechanism control problem is to design a control law v_a in terms of the armature voltage for the servomechanism to achieve accurate tracking of the input command profile $\theta_{Lc}(t)$ in terms of load position, which is generated by the guidance system in a real time, regardless the voltage noise n_v and the torque disturbance $F(.)$.

3. Basics of SISO Nonlinear Output Tracking on Sliding Modes in Canonical Space

A nonlinear MIMO system s considered

$$\begin{cases} \dot{x} = f(x,t) + \Delta f(x,t) + [B(x,t) + \Delta B(x,t)]u \\ y = h(x) \end{cases} \tag{2}$$

where $x \in R^n$, $y \in R^1$, $u \in R^1$, $f(x,t)$, $\Delta f(x,t)$, $B(x,t)$ and $\Delta B(x,t)$ are smooth functions. Here $\Delta f(x,t)$ and $\Delta B(x,t)$ represent system uncertainties and disturbances. A nominal system is

obtained when $\Delta f(x,t)=0$ and $\Delta B(x,t)=0$. The problem is to design a control function u in order to achieve a robust asymptotic tracking the command output profile $y_c(t)\ \forall i=\overline{1,m}$:

$$\lim_{t\to\infty} e = \lim_{t\to\infty}[y_c(t)-y(t)]=0. \qquad (3)$$

A sliding mode controller (SMC) design consists of two steps [1-7].

In the first step, a sliding surface is chosen such that the closed loop system motion on this surface exhibits desired behavior regardless of plant uncertainties, and disturbances.

In the second step, a control function is chosen to provide reaching of the sliding surface by the system state in finite time and to guarantee system motion in this surface thereafter. System motion on the sliding surface is called a sliding mode, and strict enforcement of the sliding mode typically leads to discontinuous high frequency switching control functions.

3.1 System transformation

Assuming the system's (2) relative degree equal to the system's order: $r=n$, the system (2) can be easily transformed to a companion form (or canonical space) [7] as follows:

$$\dot{\xi}_1=\xi_2,\quad \dot{\xi}_2=\xi_3,\ldots,\dot{\xi}_n=\varphi(x,t)+\Delta\varphi(x,t)+[b(x,t)+\Delta b(x,t)]u,\quad y=\xi_1, \qquad (4)$$

where $\varphi(x,t)+\Delta\varphi(x,t)=L_f^n(h)$, $b(x,t)+\Delta b(x,t)=L_g(L_f^{n-1}(h))$ and $L_f^n(.),L_g(.)$ are corresponding Lie derivatives. It is assumed that $b(x,t)+\Delta b(x,t)\neq 0$ in a reasonable domain $x\in\Gamma$. The functions $\Delta\varphi(x,t)$ and $\Delta b(x,t)$ reflect uncertainties and disturbances in the original system (2).

3.2 Sliding surface design

The switching surface can be designed [1-7] as follows:

$$\sigma = \sum_{i=0}^{r-1} c_i e^{(i)} = 0, \tag{5}$$

where $r = n$ is a relative degree of the system (2). The coefficients $c_i \forall i = \overline{1,n-1}$ must be identified to provide the desired eigenvalues placement to the differential equation (5). It is obvious that the systems motion on the switching surface (5) implies the robust output tracking.

3.3 Control function design

A Lyapunov-based design approach is used to derive a control law. The goal is to design such control function u that the sliding surface (5) will be reached in a finite time. Assuming $c_{n-1} = 1$ the σ - dynamics is derived as follows:

$$\dot{\sigma} = \Phi(.) - [b(x,t) + \Delta b(x,t)]u, \quad \sigma(0) = \sigma_0, \tag{6}$$

where $\Phi(.) = y_c^{(n)} + c_{n-2} e^{(n-1)} + ... + c_0 \dot{e} - \varphi(x,t) - \Delta\varphi(x,t)$.

Global asymptotic stability of the equilibrium point $\sigma = 0$ of the equation (6) will be achieved by a control law, which is designed using Lyapunov function technique. Assuming $b(x,t) > 0$ in a reasonable domain, the following candidate to a Lyapunov function is used

$$Q = \frac{b^{-1}(.)}{2}\sigma^2, \tag{7}$$

and its derivative is calculated on the trajectory of the system (6) as follows:

$$\dot{Q} = \sigma\left[-\frac{1}{2}b^{-2}(.)\dot{b}(.)\sigma + b^{-1}(.)\Phi(.) - (1+\delta)u\right], \tag{8}$$

where $\delta = \frac{\Delta b(.)}{b(.)}$. In order to provide asymptotic stability to the origin of the system (6) the following format for the derivative of the candidate to the Lyapunov function is required

$$\dot{Q} < -\rho_1|\sigma|, \quad \rho_1 > 0. \tag{9}$$

It is well known that if inequality (9) holds then the sliding surface (5) will be reached in a finite time, which can be calculated as follows:

$$t_r = \frac{|\sigma(0)|}{\rho_1}. \tag{10}$$

A following control law is designed to asymptotically stabilize $\sigma = 0$ in equation (6)

$$u = \hat{u}_{eq} + \rho \, sign\sigma, \quad \rho > 0, \tag{11}$$

where $\hat{u}_{eq}$ is an estimate the equivalent control function u_{eq}, that makes derivative of the candidate to the Lyapunov function equal to zero. The equivalent control function u_{eq} is identified from equation (8). This is

$$u_{eq} = (1+\delta)^{-1}\left[-\frac{1}{2}b^{-2}(.)\dot{b}(.)\sigma + b^{-1}(.)\Phi(.)\right]. \tag{12}$$

Remark 1. We have to use $\hat{u}_{eq}$ instead of u_{eq} in the control law (11). The reason is that the equivalent control (12) cannot be implemented because it contains uncertain terms $\Delta b(.)$, $\Delta\varphi(.)$.

Assume that the estimattion error of the equivalent control is bounded in a reasonable domain. This is

$$|\Delta u_{eq}| \le M, \tag{13}$$

where $\Delta u_{eq} = -\frac{1}{2}b^{-2}(.)\dot{b}(.)\sigma + b^{-1}(.)\Phi(.) - (1+\delta)\hat{u}_{eq}$.

Substituting equation (11) into equation (8) we can obtain the following expression:

$$\dot{Q} = \sigma\left[\Delta u_{eq} - (1+\delta)\rho sign\sigma\right] \le |\sigma|\left[M - (1+\delta)\rho\right]. \tag{14}$$

Obviously inequality (14) will fit inequality (9) if

$$\rho > \frac{M + \rho_1}{1+\delta}. \tag{15}$$

Remark 2. Inequality (15) will lead to a positive ρ if $|\delta| = \left|\frac{\Delta b(.)}{b(.)}\right| < 1$. This condition limits the value of uncertainty which the sliding mode controller (5), (11) and (15) can tolerate.

Remark 3. The sliding mode controller (5), (11) and (15) is robust, because the control amplitudes are selected on the basis of inequalities. In this case it is sufficient to know only ranges of elements of uncertain functions $|\Delta u_{eq}| \le M$ and $\left|\frac{\Delta b(.)}{b(.)}\right| < N < 1$.

Remark 4. The downside of the proposed approach is in necessity of calculation (estimation) of canonical variables of the system (4). It practically means that we need to measure or estimate controlled output and its derivatives. It can be done using asymptotic observers or sliding mode observers.

3.4 Chattering

In order to avoid a control chattering a continuous ***implementation*** of a discontinuous control law is often considered [7-9]. Usually this is an equivalent control plus a linear control law with respect to sliding surface or state variables. Very often a linear control law is taken with saturation $sat\left(\frac{\sigma_i}{\varepsilon_i}\right)$, where ε_i is a thickness of a boundary layer in $i\,th$ switching element [7-9]. Such sliding mode controllers reduce the control activity, provide a smoother operation and are free from chattering, but have some disadvantages comparing to infinity frequency switching sliding mode controllers. They are [7-9]:

1. Sliding surface can be reached only asymptotically, i.e. reaching time $\to \infty$.

2. In case of nonvanishing disturbances and uncertainties convergence is provided only to ε_i-vicinity of the sliding surface. A finite reaching time to this vicinity is guaranteed..

Commenting the first disadvantage we can say that instead of reaching time we can operate with settling time [8,9], which is finite and can be controlled by a corresponding choice of parameters of the sliding surfaces (11). Commenting the second disadvantage we can say that the distance between the system's trajectory belonging to the ε_i- vicinity of the sliding surface and the system's trajectory belonging to the sliding surfaces proportional to the size of this vicinity [1,2]. In this case we can talk about ε_i - robustness of the sliding mode with a continuous control signal. The price to pay is an eventual steady state error while the controller operates linearly in the ε_i- vicinity of the sliding surface. This problem can be addressed by the introduction of an integral term into the equation of the sliding surface (11). The continuous implementations of a sliding mode controller are widely known, for instance [10-15].

4. Basics of nonlinear output tracking on sliding modes in physical state space [4]

It is well known that control systems with sliding modes (SM) are robust to parameter uncertainties and disturbances which makes them attractive for output tracking in MIMO systems [1-3]. In order to achieve the desired output tracking, high order derivatives of the output tracking error are generally required [7]. In order to eliminate output error, multiple differentiation coordinate transformations were developed [7]. The basis transformation proposed in this work identifies such "prescribed" profiles for new state (physical) variables so that the state tracking yields the output tracking, while unmatched disturbances and nonlinearities of the original system become matched in the new basis. Conventional and dynamic sliding mode

controllers (SMC) are designed to provide the desired output tracking in a SM. The contribution of this work consists in

- the development of a nonlinear transformation of the original system with unmatched disturbances and nonlinearities into a form convenient for a SMC design,
- conventional and dynamic SMCs design for the desired output tracking. Both conventional and dynamic SMCs are insensitive to matched disturbances, but the dynamic SMC accommodates to unmatched ones.

4.1 Problem formulation

The following plant is considered:

$$\dot{x} = Ax + F(x,t) + Bu, \qquad y = Gx, \tag{16}$$

where $x \in R^n$ - a state vector; $u \in R^m$ - a control function; $y \in R^m$ - an output; A, B, G - constant matrices; $F(x,t) \in R^n$ - an unmatched disturbance, $\{A, B\}$ - a controllable pair, $rank\, B = m$, $y^*(t) \in R^m$ - reference output profile. We wish to specify a SMC

$$u_i = \begin{cases} u_i^+, \Phi_i(x, y^*, t) > 0, \\ u_i^-, \Phi_i(x, y^*, t) < 0, \quad \forall i = 1, m, \end{cases} \tag{17}$$

where $\Phi_i(x, y^*, t)$ are conventional sliding manifolds or sliding manifolds as dynamic operators, representable as transfer functions acting on some states and on output tracking errors of the system (1); u_i^+, u_i^- - continuous functions of x and t, ***to accomplish the following goals:***

- The motion of the output tracking error $e(t) = y^*(t) - y(t)$ in the SM is described by homogeneous time-invariant linear differential equations with given eigenvalues placement.
- The existence of the SM in the designed sliding manifolds must be provided.

4.2. Nonlinear transformation of the system basis

In order to eliminate the output error multiple differentiation [7], the output tracking is transformed to an equivalent state control problem. The following lemma is proved.

Lemma. The system (1) in the new basis

$$\begin{bmatrix} z^1 \\ z^2 \end{bmatrix} = \begin{bmatrix} x^{1*} \\ x^{2*} \end{bmatrix} - \begin{bmatrix} M^1 \\ M^2 \end{bmatrix} x \tag{18}$$

has the following convenient form:

$$\begin{cases} \dot{z}^1 = A^{11} z^1 + A^{12} z^2 \\ \dot{z}^2 = A^{21} z^1 + A^{22} z^2 - B^2 u + [\dot{x}^{2*} - A^{21} x^{1*} - A^{22} x^{2*} - F^2(x,t)] \\ e = G^1 z^1 + G^2 z^2; \qquad z^1 \in R^{n-m}; \quad z^2, e \in R^m. \end{cases} \tag{19}$$

where

- nonsingular linear transformation $M = \begin{bmatrix} M^1 \\ M^2 \end{bmatrix}$ has been specified as follows [1,2]:

$$MB = \begin{bmatrix} M^1 B \\ M^2 B \end{bmatrix} = \begin{bmatrix} 0 \\ B^2 \end{bmatrix}, \quad det\, B^2 \neq 0, \tag{20}$$

$$MAM^{-1} = \begin{bmatrix} A^{11} A^{12} \\ A^{21} A^{22} \end{bmatrix}, \quad \begin{bmatrix} M^1 \\ M^2 \end{bmatrix} F = \begin{bmatrix} F^1 \\ F^2 \end{bmatrix}, \quad G \begin{bmatrix} M^1 \\ M^2 \end{bmatrix}^{-1} = [G^1 : G^2]. \tag{21}$$

- x^{1*}, x^{2*} satisfy the nonlinear system of differential-algebraic equations (DAE) [4]:

$$\begin{bmatrix} I_{(n-m)\times(n-m)} & 0 \\ 0 & 0 \end{bmatrix} \begin{bmatrix} \dot{x}^{1*} \\ \dot{x}^{2*} \end{bmatrix} = \begin{bmatrix} A^{11} & A^{12} \\ G^1 & G^2 \end{bmatrix} \begin{bmatrix} x^{1*} \\ x^{2*} \end{bmatrix} + \begin{bmatrix} F^1(x,t) \\ -y^*(t) \end{bmatrix}. \tag{22}$$

Remark 1.

- The *reference state variable profiles* x^{1*}, x^{2*} are similar to "virtual control laws" in the "backstepping" method [16]. However, x^{1*} and x^{2*} are identified in one step through a solution of the system of DAE (22), which is named *the system center* [4].
- Assuming the unmatched disturbance $F^1(x,t)$ is estimated, the system (22) is solvable, if and only if, the matrix pencil $\lambda \begin{bmatrix} I_{(n-m)\times(n-m)} & 0 \\ 0 & 0 \end{bmatrix} + \begin{bmatrix} A^{11} & A^{12} \\ G^1 & G^2 \end{bmatrix}, \lambda \in R^1$ is a regular one [4].
- Implementing the concept of the "computed torque control," the system of DAE (22) is rewritten as follows:

$$\dot{x}^{1*} - A^{11}x^{1*} - A^{12}x^{2*} - F^1(x^*,t) = 0, \quad y^* - G^1x^{1*} - G^2x^{2*} = 0, \quad x^* = M^{-1}\begin{bmatrix} x^{1*} \\ x^{2*} \end{bmatrix}, \tag{23}$$

  and only the time-dependent part of the unmatched disturbance $F^1(x^*,t)$ must be estimated.
- The transformation (20) exists but is not unique if the pair $\{A, B\}$ is controllable [1,2].

4.3 Design of the conventional SMC

The following theorem is formulated and proved.

Theorem 1. Suppose that the SM exists in a conventional sliding manifold

$$\sigma = z^2 + cz^1 = 0, \quad \sigma \in R^m, \quad c \in R^{m\times(n-m)}, \tag{24}$$

then the output tracking error $e(t) = y^*(t) - y(t)$ of the system (19) in the sliding manifold (24) is described by the following linear time-invariant homogeneous system of differential equations:

$$\dot{z}^1 = (A^{11} - A^{12}c)z^1, \quad e = (G^1 - G^2c)z^1. \tag{25}$$

Proof. Substituting the equation (24) into the equations (19) yields the equations (25). ■

Remark 2. It is well known [1,2] that if the pair $\begin{bmatrix} A^{11} A^{12} \\ A^{21} A^{22} \end{bmatrix}, \begin{bmatrix} 0 \\ -B^2 \end{bmatrix}$ in the system (19) is controllable, then the pair A^{11}, A^{12} in the system (25) is also controllable. Consequently, the matrix c can be designed to provide the given eigenvalues placement to the matrix $A^{11} - A^{12}c$.

The control function (17) must be designed to provide the existence of the SM in the system (4) in the conventional sliding manifold (24). The following theorem is proved.

Theorem 2. The SM exists in the system (19) in the conventional sliding manifold (24) if

$$u = u_{eq} + \left(B^2\right)^{-1} SIGN(\sigma) \cdot R, \tag{26}$$

where $SIGN(\sigma) = diag\{sign\ \sigma_i\}$, $R = [\rho_1, \rho_2, ..., \rho_m]^T$, $\rho_i > 0 \quad i = \overline{1,m}$, and u_{eq} is identified as

$$u_{eq} = \left(B^2\right)^{-1}\left[(A^{21} + cA^{11})z^1 + (A^{22} + cA^{12})z^2 + \Phi\right], \quad \Phi = \dot{x}^{2*} - A^{21}x^{1*} - A^{22}x^{2*} - F^2(x,t). \tag{27}$$

Proof. A candidate to the Lyapunov's function

$$V = 0.5 \cdot \sigma^T \cdot \sigma > 0, \tag{28}$$

was built, and its derivative was identified as follows:

$$\dot{V} = \left(z^2 + cz^1\right)^T \left[\left(A^{21} + cA^{11}\right)z^1 + \left(A^{22} + cA^{12}\right)z^2 + \Phi - B^2 u\right]. \tag{29}$$

Substituting the formulas (26), (27) into the expression (29) yields the following inequality:

$$\dot{V} = -\sigma^T \cdot SIGN(\sigma) \cdot R = -\sum_{k=1}^{m} \rho_k \cdot |\sigma_k| < 0 \qquad \forall \rho_k > 0 \ \ \forall k = \overline{1,m}. \tag{30}$$

The equilibrium point $\sigma = 0$ is asymptotically stable. The SM exists in the surface (24). ■

Remark 3. Analyzing robustness of the SMC (24), (26), assume the equivalent control is estimated as $\hat{u}_{eq}$, and $\Delta u_{eq} = u_{eq} - \hat{u}_{eq}$, then $\dot{V} = \sum_{i=1}^{m} |\sigma_i| \left(-\rho_i + \left(\sum_{j=1}^{m} b_{ij} \Delta u_{eq_j} \right) sign\sigma_i \right)$, where

$b_{ij}\ \forall i = 1,n\ \forall j = 1,m$ are the components of the matrix B^2, and Δu_{eq_j} are the components of the vector Δu_{eq}. Apparently the SM still exists if $\rho_i > \max\left|\sum_{j=1}^{m} b_{ij}\Delta u_{eq_j}\right| \quad \forall i = 1,n$.

4.4 Design of the dynamic SMC

Assume the unmatched disturbance $F^1(x,t)$ is estimated as $\hat{F}^1(x,t)$, and $\Delta F^1(x,t) = F^1(x,t) - \hat{F}^1(x,t)$. Then the system (16) is described in the new basis

$$\begin{cases} \dot{z}^1 = A^{11}z^1 + A^{12}z^2 - \Delta F^1(x,t), \\ \dot{z}^2 = A^{21}z^1 + A^{22}z^2 - B^2u + [\dot{x}^{2*} - A^{21}x^{1*} - A^{22}x^{2*} - F^2(x,t)], \\ e = G^1z^1 + G^2z^2; \qquad z^1 \in R^{n-m};\ \ z^2, e \in R^m. \end{cases} \tag{31}$$

In order to reduce the effect of a remaining part of the unmatched disturbance $\Delta F^1(x,t)$ to the output steady state tracking error, the dynamic sliding manifold [4-6] was designed as *a linear dynamic operator* acting on some states and on output tracking errors [4-6] as follows:

$$\Im(z^2, e) = z^2 + W(s)e = \left[I : W(s)\right] \cdot \begin{bmatrix} z^2 \\ e \end{bmatrix}, \tag{32}$$

where

$s = d/dt,\quad W(s) = \left[W_{i,j}(s)\right],\quad W_{i,j}(s) = P_{m_{i,j}}(s)/Q_{n_{i,j}}(s) \quad \forall i = 1,m\ \forall j = 1,m;\quad P_{m_{i,j}}(s),\ Q_{n_{i,j}}(s)$

are polynomials of s and $m_{i,j} \le n_{i,j}$. The following theorem is formulated and proved.

Theorem 3. Suppose that the SM exists in the system (31) in the sliding manifold

$$\Im(z^2, e) = 0. \tag{33}$$

then the output tracking error e in the system (31) in the dynamic sliding manifold (33) is described by the operator equation

$$\left[I + G^2W(s) + G^1(sI - A^{11})^{-1}A^{12}W(s)\right]e = -G^1(sI - A^{11})^{-1}\Delta F^1(x,t). \quad (34)$$

Proof. Assume the SM exists in the system (31) in the dynamic sliding manifold (33), and substitute (32), (33) into (31) to obtain (34).

Remark 4. In order to provide asymptotic output tracking in the SM, the operator polynomials $P_{m_{i,j}}(s), Q_{n_{i,j}}(s)$ $\forall i = \overline{1,m}\ \forall j = \overline{1,m}$ must be identified to guarantee the given eigenvalues placement and to reject the effect of the disturbance $\Delta F^1(x,t)$ on the output steady state tracking error. The nonlinear function $\Delta F^1(x,t)$ can be approximated by the time-function $\Delta F^1(x^*(t),t)$, where $x^*(t)$ is the reference state of (23). The disturbance rejection condition $\lim_{t\to\infty} sE(s) = 0$ can be easily met by a corresponding choice of the polynomials $P_{m_{i,j}}(s), Q_{n_{i,j}}(s)$. The control function (17) must be designed to ensure the existence of the SM in the system (31) in the dynamic sliding manifold (33). The following theorem is formulated and proved.

Theorem 4. The SM exists in the system (31) in the dynamic sliding manifold (33), if

$$u = u_{eq} + \left(B^2\right)^{-1} \cdot \left(I + W(s)G^2\right)^{-1} \cdot SIGN(\Im) \cdot \Gamma, \quad (35)$$

where $SIGN(\Im) = diag\{\ sign\ \Im_i\}$ and $\Gamma = \left[\rho_1, \rho_2, \ldots, \rho_m\right]^T$, $\rho_i > 0 \quad i = \overline{1,m}$ are arbitrary chosen constants, and u_{eq} is the following equivalent control function [1,2]:

$$u_{eq} = \left(B^2\right)^{-1} \cdot \left(I + W(s)G_2\right)^{-1} \cdot [(A^{21} + W(s)G^1A^{11} + W(s)G^2A^{21})z^1 + (A^{22} + W(s)G^1A^{12} + W(s)G^2A^{22})z^2 + \\ + (I + W(s)G^2)\Phi - W(s)G^1\Delta F^1], \quad \Phi = \dot{x}^{2*} - A^{21}x^{1*} - A^{22}x^{2*} - F^2(x,t). \quad (36)$$

Proof. A candidate for the Lyapunov's function

$$V = 0.5(\Im)^T \Im > 0, \quad (37)$$

was built, and its derivative was identified on the states of the system (31) as follows:

$$\dot{V} = \Im^T \dot{\Im} = \Im^T [(A^{21} + W(s)G^1 A^{11} + W(s)G^2 A^{21}) z^1 + (A^{22} + W(s)G^1 A^{12} + W(s)G^2 A^{22}) z^2 + \\ + (I + W(s)G^2)\Phi - W(s)G^1 \Delta F^1 - (1 + W(s)G^2) B^2 u]. \tag{38}$$

Substituting formulas (35) and (36) into the expression (38) the following expression is obtained:

$$\dot{V} = -\Im^T \cdot SIGN(\Im) \cdot \Gamma = -\sum_{i=1}^{m} \rho_i \mid \Im_i \mid < 0 \quad \forall \rho_i > 0. \tag{39}$$

Hence, that the manifold $\Im = 0$ is "attractive" (or equilibrium point $\Im = 0$ is stable), and the SM exists in the dynamic sliding manifold (32), (33) in the system (31). ■

4.5 Example

Suppose we have a nonlinear control system

$$\begin{cases} \dot{x}_1 = x_2, \quad \dot{x}_2 = -x_2 - x_3 + x_1^2 + f_1(t), \quad \dot{x}_3 = x_3 + \sin x_1 + f_2(t) + 10u \\ y = x_1 \end{cases} \tag{40}$$

with unknown smooth matched $| f_2(t) | \le 3$ and unmatched $| f_1(t) | \le 3$ disturbances.

We wish the output $y(t)$ to asymptotically track a reference profile $y^*(t)$. That is

$$\lim_{t \to \infty} |y^*(t) - y(t)| = \lim_{t \to \infty} |e(t)| = 0 \tag{41}$$

The new basis variables (18) in the system (40) have been introduced as follows:

$$z_1 = x_1^* - x_1, \; z_2 = x_2^* - x_2, \; z_3 = x_3^* - x_3. \tag{42}$$

Assuming $\Delta F^1(x,t)$ and $f_1(t)$ are known, the equations of the system center (21) are written as follows:

$$\dot{x}_1^* = x_2^*, \; \dot{x}_2^* = -x_2^* - x_3^* + x_1^2 + f_1(t), \; y^*(t) = x_1^*. \tag{43}$$

The solution to the equations of the system center (43) was identified. This is

$$x_1^*(t) = y^*(t), \quad x_2^* = \dot{y}^*(t), \quad x_3^*(t) = -\ddot{y}^*(t) - \dot{y}^*(t) + x_1^2 + f_1(t). \tag{44}$$

The following expression for the conventional sliding manifold was obtained:

$$\sigma = z_3 - 29z_2 - 210z_1 = -\dddot{y}^*(t) - 30\ddot{y}^*(t) + x_1^2 - 210\dot{y}^*(t) + f_1(t) - x_3 + 29x_2 + 210x_1 \,. \qquad (45)$$

The control law (26), (45) was designed with $\left(B^2\right)^{-1}\rho = 0.75$, and the equivalent control $u_{eq} = -0.1\dddot{y}^* - 3\ddot{y}^* + 0.2x_1x_2 - 0.1\dot{f}_1 - 21\dot{y}^* + 2.9f_1 - 0.1f_2 - 3x_3 + 18.1x_2 - 0.1\sin x_1 + 2.9x_1^2$. The system (40) was simulated with the SMC $u = \hat{u}_{eq} + \left(B^2\right)^{-1}\rho\, sign\,\sigma$, where $\hat{u}_{eq} = K_{eq}(t)u_{eq}$ and $K_{eq}(t)$ is an uncertain gain. The results of the simulation show the perfect output tracking, which is insensitive to matched and unmatched disturbances, and to $K_{eq}(t) \in [0.7, 1.4]$.

Assuming the unmatched disturbance $f_1(t)$ is unknown, the simulation was repeated without $f_1(t)$ in the sliding surface (45). The output tracking exhibits the stable output tracking with the non-zero output steady state error. In order to nullify the output steady state error, assuming $\lim_{t\to\infty} f_1(t) = const$, the dynamic sliding manifold was designed as

$$\Im = -\dddot{y}^*(t) - \ddot{y}^*(t) + x_1^2 - x_3 - W(s)e\,, \quad W(s) = \frac{1000(s^2 + 8s + 3)}{s(s + 50)}. \qquad (46)$$

The results of the simulation of the system (40) with the dynamic SMC (35), (46) show that the output tracking error has a zero steady state value and is insensitive to the matched disturbance. $f_2(t)$. Hence, the dynamic SMC joins features of a conventional compensator (accommodation to unmatched disturbances) and a conventional SMC (insensitivity to matched disturbances).

4.6 Conclusion

Nonlinear output tracking in MIMO systems with unmatched nonlinearities and disturbances is considered in SMs. The system is nonlinearly transformed to a form convenient for SM synthesis. Both conventional and dynamic SMCs are designed. In both cases, only the time-dependent part of the unmatched disturbance must be estimated. Results show that both

controllers are insensitive to match disturbances: however, dynamic SMC accommodates to unmatched disturbances. Future research will involve the chattering elimination and discrete realization of the designed SMCs, as well. The developed approach will be extended to a nonminimal phase nonlinear output tracking. Preliminary results look promising.

5. Finite-reaching-time continuous SMC for MIMO nonlinear systems [17]

Sliding mode control is a nonlinear robust control technique, which is actively developing during last 30-35 years [1,2]. Since the closed-loop system exhibits he desired robust performance moving on the sliding surface, it is highly desirable to reach the sliding surface in a finite time. The system's motion on the sliding surface is called the sliding mode. Historically, sliding modes were discovered in variable structure systems, which feedback structure changes depending on value of a state vector to drive the system's trajectory onto the "custom-made" sliding surface. While on the surface the variable structure control yields an infinity frequency switching control [1,2], which is practically unrealizable in many cases. Dynamics of switching elements and finite sampling time of microprocessors prevent from implementation of infinity frequency switching control law and lead to so called control chattering (limit cycles with finite frequency oscillation in a closed-loop system). Employing a two-loop structure of a sliding mode controller [14,15] it is impossible to have a high frequency switching controller in the outer loop. Outer loop controller produces a profile that must be followed in the inner loop. Of course, this profile must be continuous. In the work [17] a continuous sliding mode controller is proposed as a specific type of a sliding mode controller, but not as implementation of a discontinuous high frequency switching control law. Robustness of the designed controller, which is an issue of

crucial importance, is addressed as well. Theoretical results are validated via computer simulations.

5.1 Problem formulation

Consider the nonlinear square MIMO system

$$\begin{cases} \dot{x} = f(x) + G(x)u \\ y = h(x) \end{cases} \tag{47}$$

where $x \in R^n$, $y \in R^m$, $u \in R^m$. Assume that the functions $f(x)$, $h(x)$ are smooth vector fields, and columns $g_i(x)$ $\forall i = \overline{1,m}$ of the matrix $G(x) \in R^{n \times m}$ are smooth vector fields as well. Assume also that the system (1) is completely linearizable in a reasonable domain $x \in \Gamma$, i.e. the system (47) does not have internal (zero) dynamics.

Given in real time an output reference profile $y_r(t)$ identify a continuous sliding mode controller which

1. provides a given eigenvalues to the de-coupled output tracking error performance in the sliding mode,
2. drives the closed-loop system trajectory to the sliding surface in a finite time.

5.2 Basis Transformation

Differentiating the outputs, the system (47) can be easily transformed to a normal (canonical) form [7]

$$\begin{bmatrix} y_1^{(r_1)} \\ y_2^{(r_2)} \\ \dots\dots \\ y_m^{(r_m)} \end{bmatrix} = \begin{bmatrix} L_f^{r_1} h_1(x) \\ L_f^{r_2} h_2(x) \\ \dots\dots\dots\dots \\ L_f^{r_m} h_m(x) \end{bmatrix} + E(x)u \tag{48}$$

where

$$E(x) = \begin{bmatrix} L_{g_1}(L_f^{r_1-1}h_1) & L_{g_2}(L_f^{r_1-1}h_1) \dots L_{g_m}(L_f^{r_1-1}h_1) \\ L_{g_1}(L_f^{r_2-1}h_2) & L_{g_2}(L_f^{r_2-1}h_2) \dots L_{g_m}(L_f^{r_2-1}h_2) \\ \dots\dots\dots\dots & \\ L_{g_1}(L_f^{r_m-1}h_2) & L_{g_2}(L_f^{r_m-1}h_m) \dots L_{g_m}(L_f^{r_m-1}h_m) \end{bmatrix}, \quad |E(x)| \neq 0 \; \forall x \in \Gamma: \quad L_f^{r_i} h_i \text{ and } L_{g_i}(L_f^{r_i-1}h_i)$$

$\forall i = \overline{1,m}$ are corresponding Lie derivatives.

5.3 Terminal attractor

A useful result is formulated in a following Lemma.

Lemma. The origin of a differential equation

$$\dot{z} = -\omega z^a, \quad z(0) > 0, \omega > 0 \tag{49}$$

is a terminal attractor with a finite reaching time

$$t_r = \frac{(z(0))^{1-a}}{\omega(1-a)} \quad \forall a \in (0,1). \tag{50}$$

Indeed, integrating (49) we have obtained

$$(z(t))^{1-a} = (z(0))^{1-a} - (1-a)\omega t. \tag{51}$$

Requiring $z(t_r)=0$ implies formula (50).

5.4 A finite-reaching time continuous sliding mode controller design

Achieving de-coupled output tracking error performance in the sliding mode, the following sliding surfaces are designed

$$\sigma_i = e_i^{(r_i-1)} + c_{i,r_i-2}e_i^{(r_i-2)} + ... + c_{i,1}e_i^{(1)} + c_{i,0}e_i\,,\ \forall i = \overline{1,m}, \tag{52}$$

where $e_i = y_{r,i}(t) - y_i(t)$, $e_i^{(j)} = \dfrac{d^j e_i}{dt^j}$ and the coefficients $c_{i,j}\ \forall i = \overline{1,m} \forall j = \overline{0,r_i-2}$ are chosen to provide given eigenvalues placement to the de-coupled differential equations $\sigma_i = 0$ $\forall i = \overline{1,m}$.

Designing a continuous sliding mode controller for the system (48) we need to provide asymptotic stability to its motion in the σ-subspace, which is described as follows:

$$\dot{\sigma} = \Psi(.) - E(x)u\,, \tag{53}$$

where

$$\Psi(.) = \{\psi_1(.), \psi_2(.), ..., \psi_m(.)\}^T,\ \psi_i(.) = y_{r,i}^{(r_i)}(t) + c_{i,r_i-2}e_i^{(r_i-1)} + ... + c_{i,0}e_i^{(1)} - L_f^{r_i}h_i(x)\ \ \forall i = \overline{1,m}. \tag{54}$$

Introducing a new control variable

$$\tilde{u} = E(x)u\,, \tag{55}$$

the system (53) can be rewritten in a scalar format. This is

$$\dot{\sigma}_i = \psi_i(.) - \tilde{u}_i\ \ \forall i = \overline{1,m}. \tag{56}$$

The system (56) is obviously input-output de-coupled. Hence, analyzing stability of the origin of the system (56), we can analyze stability of each i^{th} equation $\forall i = \overline{1,m}$. Candidates to Lyapunov functions are introduced. They are

$$V_i = \frac{1}{2}\sigma_i^2. \tag{57}$$

We will look for the derivative of the candidates to Lyapunov functions (57) in the following format:

$$\dot{V}_i = -\omega_i V_i^{a_i},\ \ a_i > 0, \omega_i > 0\,. \tag{58}$$

Then, applying Lemma we can conclude that the origin of the i[th] equation of the system (56) will be reached in a finite time $\forall i = \overline{1,m}$

$$t_{r_i} = \frac{(V_i(0))^{1-a_i}}{\omega_i(1-a_i)} \quad \forall a_i \in (0,1)\,. \tag{59}$$

It means that $\sigma_i = 0 \;\; \forall i = \overline{1,m}$ become terminal attractors. Substituting expressions (52) and (56) into formulas (57), a control function $\tilde{u}$ is identified as follows:

$$\tilde{u} = -\Psi(.) + R \cdot \Sigma, \tag{60}$$

where $R = diag\left\{\frac{\omega_i}{2^{a_i}}\right\} \forall i = \overline{1,m}$; $\Sigma = \left\{\sigma_1^{2a_1-1}, \sigma_2^{2a_2-1}, ..., \sigma_m^{2a_m-1}\right\}^T$.

Substituting equation (60) into equations (56), we obtained equations of the closed-loop system's (48) motion in the σ-subspace. They are

$$\dot{\sigma}_i = -2^{-a_i}\omega_i\sigma^{2a_i-1} \quad \forall i = \overline{1,m}. \tag{61}$$

Making coordinates of the control function (14) continuous and avoiding singularity in the origin of the system (61), we will look for the parameters "a_i" in the following format:

$$a_i = \frac{p_i}{q_i} \quad \forall i = \overline{1,m}, \tag{62}$$

where p_i and q_i are integer numbers. Since σ_i can be either positive or negative the values of q_i and $2p_i - q_i > 0$ must be odd. Hence, the parameters p_i and q_i must meet the following conditions

$$p_i, q_i \in \Omega_i: \left\{p_i, q_i \middle| 2p_i > q_i,\;\; p_i < q_i,\;\; q_i \text{ is odd}\right\} \forall i = \overline{1,m}. \tag{63}$$

As soon as the values of the parameters p_i and q_i have been identified in accordance with the conditions (63) the value of the parameters ω_i must be chosen to achieve a given reaching times (59).

The original finite-reaching-time continuous sliding mode control law u has been identified in accordance with formulas (55) and (60) as follows:

$$u = E(x)^{-1}\left[-\Psi(.) + R \cdot \Sigma\right]. \tag{64}$$

The obtained results are formulated into the following Theorem.

Theorem. The sliding surfaces (56) will be reached in finite times (59) via the continuous sliding mode controller (64) if values of parameters "a_i" are chosen in accordance with formulas (60) and (63).

5.5 Robustness

Assuming

$$\Psi(.) = \Psi_0(.) + \Delta\Psi(.),\ E(x) = E_0(x) + \Delta E(x), \tag{65}$$

where $\Delta\Psi(.)$ and $\Delta E(x)$ are uncertain vector and matrix correspondingly. Designing control (64) in the following format

$$u = E_0(x)^{-1}\left[-\Psi_0(.) + R \cdot \Sigma\right], \tag{66}$$

and substituting expression (66) into equations (53), we obtained

$$\dot{\sigma} = \Delta\Psi(.) - \Delta M \cdot \Psi_0(.) - (I + \Delta M)R \cdot \Sigma, \tag{67}$$

where $\Delta M = \Delta E(x) \cdot E_0^{-1}(x)$.

Equation (67) is rewritten in a scalar format. This is

$$\dot{\sigma}_i = \Delta\psi_i(.) - \left(\Delta M \cdot \Psi_0(.)\right)_i - \frac{\omega_i}{2^{a_i}}\sigma_i^{2a_i-1} - \sum_{j=1}^{m}\Delta M_{ij}\frac{\omega_j}{2^{\omega_j}}\sigma_j^{2a_j-1} \quad , \forall i = \overline{1,m} \; . \tag{68}$$

Substituting equations (68) into equations (57), we obtained

$$\dot{V}_i = -\left[\omega_i(1+\Delta M_{ii}) + \frac{2^{a_i}\left(-\Delta\psi_i(.) + \left(\Delta M \cdot \Psi_0(.)\right)_i + \sum_{\substack{j=1 \\ j\neq i}}^{m}\Delta M_{ij}\frac{\omega_j}{2^{\omega_j}}\sigma_j^{2a_j-1}\right)}{\sigma_i^{2a_i-1}}\right]V_i^{a_i} \; . \tag{69}$$

Assuming

$$\left|\Delta M_{ii}\right| \le L_{ii} < 1, \; \left|\Delta M_{ij}\right| \le L_{ij}, \; \left|\Delta\psi_i\right| \le R_i, \; \left|\left(\Delta M \cdot \Psi_0(.)\right)_i\right| \le G_i, \; \left|\sigma_j\right| \le \pi_j \quad \forall i = \overline{1,m} \; \forall j = \overline{1,m} \tag{70}$$

we introduce positive constants

$$\Phi_i = R_i + G_i + \sum_{\substack{j=1 \\ j\neq i}}^{m}\frac{\omega_j}{2^{a_j}}L_{ij}\pi_j^{2a_j-1} \; . \tag{71}$$

Transforming equations (69) taking into account expressions (60) and (71) we obtained

$$\dot{V}_i \le -\left[\omega_i(1-L_{ii}) - \frac{2^{a_i}\Phi_i}{\left|\sigma_i^{2a_i-1}\right|}\right]V_i^{a_i} \quad \forall i = \overline{1,m} \; . \tag{72}$$

Inequalities (72) are rewritten in a format

$$\dot{V}_i \le -\tilde{\omega}_i V_i^{a_i} \quad \forall i = \overline{1,m} \; , \tag{73}$$

where

$$\tilde{\omega}_i = \frac{\left(V_i(0)\right)^{1-a_i}}{t_{r_i}(1-a_i)} \; , \forall i = \overline{1,m} \tag{74}$$

and

$$\omega_i(1-L_{ii})-\frac{2^{a_i}\Phi_i}{\left|\sigma_i^{2a_i-1}\right|}\geq\tilde{\omega}_i\ \ \forall i=\overline{1,m}. \tag{75}$$

Inequalities (75) actually form domains where conditions (73) are met. It means that the following domains

$$|\sigma_i|\leq\left(\frac{2^{a_i}\Phi_i}{\omega_i(1-L_{ii})-\tilde{\omega}_i}\right)^{\frac{1}{2a_i-1}}\ \ \forall i=\overline{1,m} \tag{76}$$

will be reached by the trajectories σ_i in given finite times (59), and trajectories σ_i will stay in these domains thereafter. Hence, solutions of the closed loop systems (68) are uniformly ultimately bounded [8]. What is remarkable, that choosing values of the parameters ω_i to meet inequalities

$$\omega_i>\frac{2^{a_i}\Phi_i+\tilde{\omega}_i}{1-L_{ii}}\ \ \forall i=\overline{1,m} \tag{77}$$

and making $2a_i-1$ arbitrary small, we can make a size of the attractivity domains (76) arbitrary small as well, retaining the control law (66) continuous. In order to achieve a similar result, using linear/saturation approximation of a discontinuous sliding mode controller, a gain of such controller must be arbitrary large [7,8], which is impractical. Hence, a designed continuous sliding mode controller is extremely robust.

5.6 Example

A nonlinear MIMO system is considered

$$\begin{cases} \dot{x}_1 = x_2 \\ \dot{x}_2 = \cos x_3 + \left(x_1^2 + 1\right)u_1 + u_2 + f_1(t) \\ \dot{x}_3 = \sin x_1 + 0.5u_1 + \left(x_2^2 + 1\right)u_2 + f_2(t) \\ y_1 = x_1, \;\; y_2 = x_3 \end{cases} \tag{78}$$

Functions $f_i(t) : |f_i(t)| \le \eta_i \;\; \forall i = 1,2$ are unknown, bounded, matched disturbances. The system (78) is completely linearizable with a vector-relative degree $r = \{2,1\}$. The system (78) is transformed [1,2,7] into the normal format (48) as follows:

$$\begin{bmatrix} \ddot{y}_1 \\ \dot{y}_2 \end{bmatrix} = \begin{bmatrix} \cos x_3 \\ \sin x_1 \end{bmatrix} + \begin{bmatrix} f_1(t) \\ f_2(t) \end{bmatrix} + \begin{bmatrix} \left(x_1^2 + 1\right) & 1 \\ 0.5 & \left(x_2^2 + 1\right) \end{bmatrix} \begin{bmatrix} u_1 \\ u_2 \end{bmatrix}. \tag{79}$$

The goal is to design a robust, continuous sliding mode controller to provide de-coupled tracking of smooth output reference profiles $y_{1r}(t)$ and $y_{2r}(t)$ in finite-reaching-time sliding modes.

The sliding surfaces are designed in the format (52) as follows

$$\sigma_1 = \dot{e}_1 + 5e_1, \quad \sigma_2 = e_2, \tag{80}$$

where $e_1 = y_{1r} - y_1$, $e_2 = y_{2r} - y_2$.

The parameters p_i, q_i and ω_i are identified $\forall i = 1.2$. They are

$$p_1 = p_2 = 2, \quad q_1 = q_2 = 3, \quad \omega_1 = 16, \quad \omega_2 = 10 \;.$$

The continuous "cubic root" sliding mode controller is designed in the format (64) as follows:

$$\begin{bmatrix} u_1 \\ u_2 \end{bmatrix} = \begin{bmatrix} \dfrac{x_2^2 + 1}{\left(x_1^2 + 1\right)\left(x_2^2 + 1\right) - 0.5} & -\dfrac{1}{\left(x_1^2 + 1\right)\left(x_2^2 + 1\right) - 0.5} \\ -\dfrac{0.5}{\left(x_1^2 + 1\right)\left(x_2^2 + 1\right) - 0.5} & \dfrac{x_1^2 + 1}{\left(x_1^2 + 1\right)\left(x_2^2 + 1\right) - 0.5} \end{bmatrix} \begin{bmatrix} \tilde{u}_1 \\ \tilde{u}_2 \end{bmatrix}, \tag{81}$$

where

$$\begin{cases} \tilde{u}_1 = \ddot{y}_{1r} + 5\dot{y}_{1r} - \cos x_3 - 5x_2 + 10.0\sqrt[3]{\sigma_1} \\ \tilde{u}_2 = \dot{y}_{2r} - \sin x_1 + 6.3\sqrt[3]{\sigma_2} \end{cases} \tag{82}$$

The system (78) was simulated with the continuous "cubic root" sliding mode controller (82) and with the continuous "linear" sliding mode controller

$$\begin{cases} \tilde{u}_1 = \ddot{y}_{1r} + 5\dot{y}_{1r} - \cos x_3 - 5x_2 + 16\sigma_1, \\ \tilde{u}_2 = \dot{y}_{2r} - \sin x_1 + 20\sigma_2. \end{cases} \tag{83}$$

It is worth to note that gains before the σ – terms in formula (83) are increased from 10 to 16 and from 6.3 to 20 comparing with formula (82), which helps the "linear" controller (83) to be more aggressive.

The following initial conditions and the reference profiles were used

$$x_1(0) = 0.2,\ x_2(0) = 0.1,\ x_3(0) = -0.15,\ y_{1r}(t) = 0.5\sin t,\ \ y_{2r}(t) = 0.5\cos t. \tag{84}$$

Simulations confirm a finite-reaching time property of the designed continuous sliding mode controller and show improving robustness comparing with "linear" sliding mode controller.

6. Concepts for a Control System Development

Engineering analysis is performed to investigate the implementation of a sliding mode controller algorithm that will reduce sensitivity to feedback noise in Control Actuation Systems (CAS) such as those used on Guided MLRS, Low Cost Precision Kill (LCPK), and Compact Kinetic Energy Missile (CKEM). The GFE model of the CAS is used to demonstrate performance enhancement achieved with the sliding mode controller for a variety of potential noise sources. Two control systems are designed.

First. The "nested" structure of the control system is developed. Employing backstepping concepts [16] the outer loop controller is designed, in particular, as a continuous finite-reaching time SMC, using continuous sliding mode control technique [7-9,17]. Armature current is

treated as a virtual control in the outer loop sliding mode controller. Armature current command, which is formed in the outer loop by a continuous finite-reaching-time SMC [17] in order to provide an asymptotic tracking of the load position angle, is tracked in the inner loop. The inner loop controller is designed in order to follow armature current command. The inner loop high frequency switching SMC is designed in terms of armature voltage. This design concept is based on assumption that compensated dynamics of the inner (current) loop is much faster then the compensated dynamics of the outer (position) loop. Advantage of the two loop SMC is that sliding surfaces are of reduced order and the disturbance $F(.)$ is matched [1,2]. It means that the SMC will compensate for the disturbance $F(.)$ without its measurement or estimation. Implementation of the SMC is considered in a relay format and in a pulse-width-modulator (PWM) format.

Second. Single loop SMC is designed using the system center design technique, which is discussed in the chapter 4. Advantage of this approach is in simpler structure (single loop) of the sliding mode controller. The single loop high frequency switching SMC is designed in terms of armature voltage. Implementation of the SMC is considered in a relay format and in a pulse-width-modulator (PWM) format. Sliding mode observer is designed to estimate disturbance $F(.)$ that is unmatched in this case.

7. Two loop sliding mode controller design

Designing a two-loop SMC for the servomechanism (1), we start with the outer loop continuous finite-reaching-time SMC design.

7.1 Outer Loop Continuous Finite-Reaching-Time SMC Design

The mathematical model describing the "armature current - load position" relationship is derived from equation (1). This is

$$\begin{cases} \dfrac{d\theta_L}{dt} = \dfrac{1}{n_g}\omega_m \\ \dfrac{d\omega_m}{dt} = \dfrac{1}{J}\left[k_t i_a - F(.)\right] \\ y = \theta_l \end{cases} \tag{85}$$

Assuming the load position reference profile $\theta_{Lc}(t)$ is given in real time, the problem is to design a continuous virtual sliding mode controller $i_{ac}(t)$ achieving an asymptotic tracking

$$\lim_{t\to\infty}\left|\theta_{Lc}(t) - \theta_L(t)\right| = 0. \tag{86}$$

At the first step of the outer loop SMC design the sliding surface is identified as follows:

$$\sigma = \dot{e} + 200e, \qquad e = \theta_{Lc} - \theta. \tag{87}$$

While on the surface (87) the system (85) will exhibit the following tracking behavior:

$$e(t) = e(t_o)\exp(-200t), \tag{88}$$

that is insensitive to disturbance $F(.)$.

At the second step the continuous finite-reaching-time virtual SMC law i_{ac} is designed to asymptotically stabilize $\sigma = 0$. The sliding surface dynamics is described as follows:

$$\dot{\sigma} = \ddot{\theta}_{Lc} + 200\dot{\theta}_{Lc} - 1.588\omega_m + 625.2F(.) - 278.2i_{ac}. \tag{89}$$

The equivalent control $i_{ac\,eq}$ that achieves the system's (85) motion in the sliding surface $\sigma = 0$ is identified

$$i_{ac\,eq} = 0.0036\ddot{\theta}_{Lc} + 0.719\dot{\theta}_{Lc} - 0.057\omega_m + 2.25F(.). \tag{90}$$

The disturbance $F(.)$ is omitted while equivalent control is estimated. This is

$$\hat{i}_{ac\,eq} = 0.0036\ddot{\theta}_{Lc} + 0.719\dot{\theta}_{Lc} - 0.057\omega_m. \tag{91}$$

The continuous finite-reaching -time SMC is designed in the format of equation (66) to achieve the origin of the equation (89). In the other words, existence of the sliding mode will be provided. This is

$$i_{ac} = \hat{i}_{ac\,eq} - \frac{\omega}{2^a}\sigma^{\hat{2}a-1}, \tag{92}$$

where $a = \frac{2}{3}$ and $\omega = 8$. As a result the control law (91), (92) is obtained

$$i_{ac} = 0.0036\ddot{\theta}_{Lc} + 0.719\dot{\theta}_{Lc} - 0.057\omega_m - 5\sqrt[3]{\sigma}\,. \tag{93}$$

It is expected that the outer loop SMC will have enhanced robustness, as discussed in the chapter 5.

7.2 Inner Loop SMC Design

The mathematical model describing the "armature voltage - armature current" relationship is derived from equation (1). This is

$$\begin{cases} \frac{di_a}{dt} = \frac{1}{L_a}\left[v_a + n_v - R_a i_a - k_b\omega_m\right] \\ y = i_a \end{cases}. \tag{94}$$

Having the load armature current command profile $i_{ac}(t)$ (93) given in real time, the problem is to design a SMC $v_a(t)$ achieving an asymptotic tracking

$$\lim_{t\to\infty}\left|i_{ac}(t) - i_a(t)\right| = 0. \tag{95}$$

At the first step of the inner loop SMC design the sliding surface is identified as follows:

$$s = \eta, \qquad \eta = i_{ac}(t) - i_a(t). \tag{96}$$

While on the surface (96) the system (94) will exhibit the perfect tracking behavior:

$$i_a(t) = i_{ac}(t), \tag{97}$$

that is insensitive to the voltage noise n_v.

At the second step the SMC law v_a is designed to asymptotically stabilize $s = 0$. The sliding surface dynamics is described as follows:

$$\dot{s} = \dot{i}_{ac} + 2778 i_a + 13.0\omega_m + 277.8 n_v - 277.8 v_a. \tag{98}$$

The equivalent control $i_{ac\,eq}$ is identified

$$v_{a\,eq} = 0.0036\dot{i}_{ac} + 10 i_a + 0.0503\omega_m + n_v. \tag{99}$$

Simplifying the control law, equivalent control is estimated at zero level. The inner loop SMC is designed in the format of equation (11) to achieve the origin of the equation (98). In the other words, existence of the sliding mode will be provided. This is

$$v_a = \rho \; sign\, s, \tag{100}$$

where

$$\rho > \left| 0.0036\dot{i}_{ac} + 10 i_a + 0.0503\omega_m + n_v \right|. \tag{101}$$

In accordance to physical limitation to the armature voltage the SMC (100) is chosen as follows:

$$v_a = 31 \; sign\, s. \tag{102}$$

Inequality (101) becomes

$$\left| 0.0036\dot{i}_{ac} + 10 i_a + 0.0503\omega_m + n_v \right| < 31, \tag{103}$$

and gives a domain of existence of sliding mode on the surface (96).

7.3 Simulation of the servomechanism with two loop SMC

The system (1) was simulated with the two-loop SMC (87), (93), (96), (100). Nonlinearities were taken into account. Backlash characteristic of the gear train was used with 0.75 width, and the deadband block was used with the deadband equal to 3.0 (fig. 1). The first set of simulations was performed for $\theta_{Lc} = 0.2 sign(\sin t)$. The results of simulations are shown in figures 3-9. Modeling the noise voltage n_v we assume that armature current discontinuity, which is caused by switching control voltage v_a, leads to the noise voltage n_v. During simulation the noise voltage n_v is modeled as follows: $n_v = 4 \cdot 10^{-4} \frac{dv_a}{dt}$. Differentiation is performed numerically.

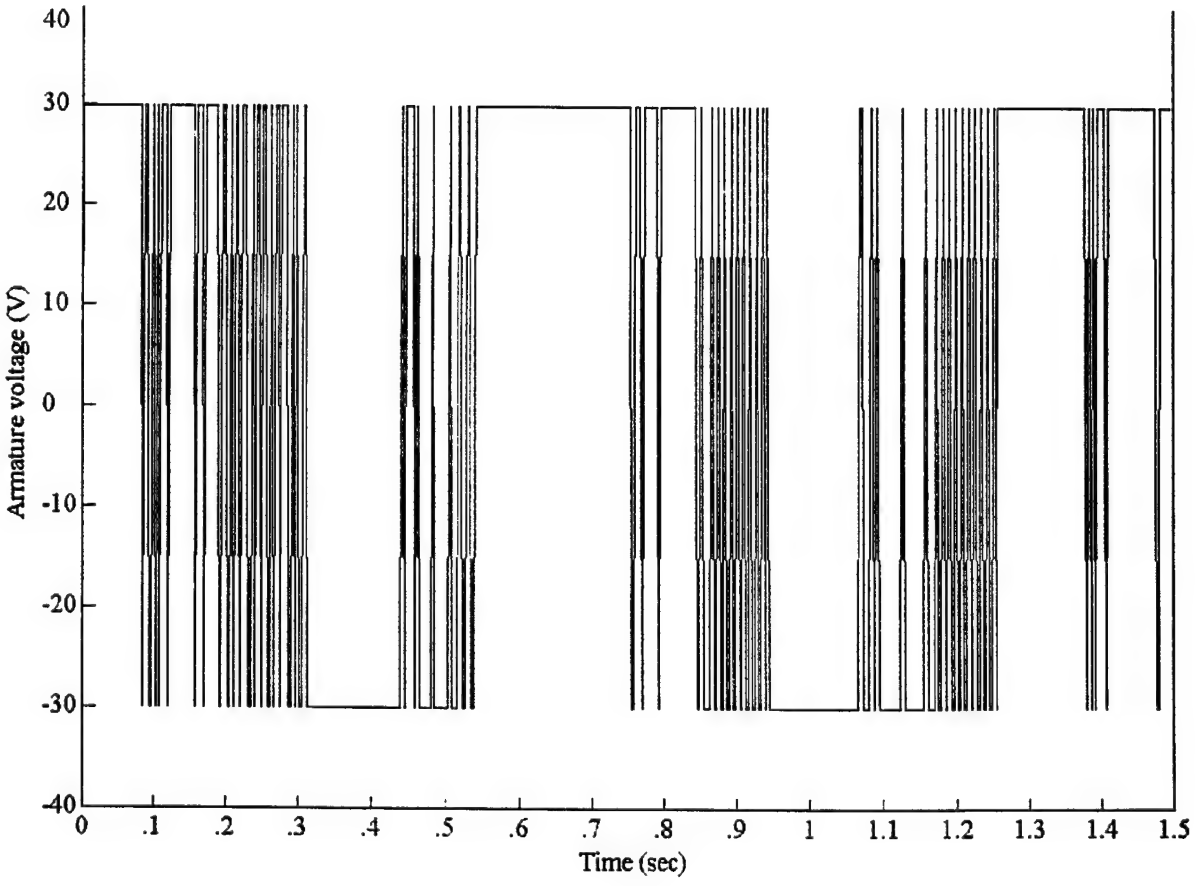

Fig.3 Armature voltage v_a ($\theta_{Lc} = 0.2 sign(\sin t)$)

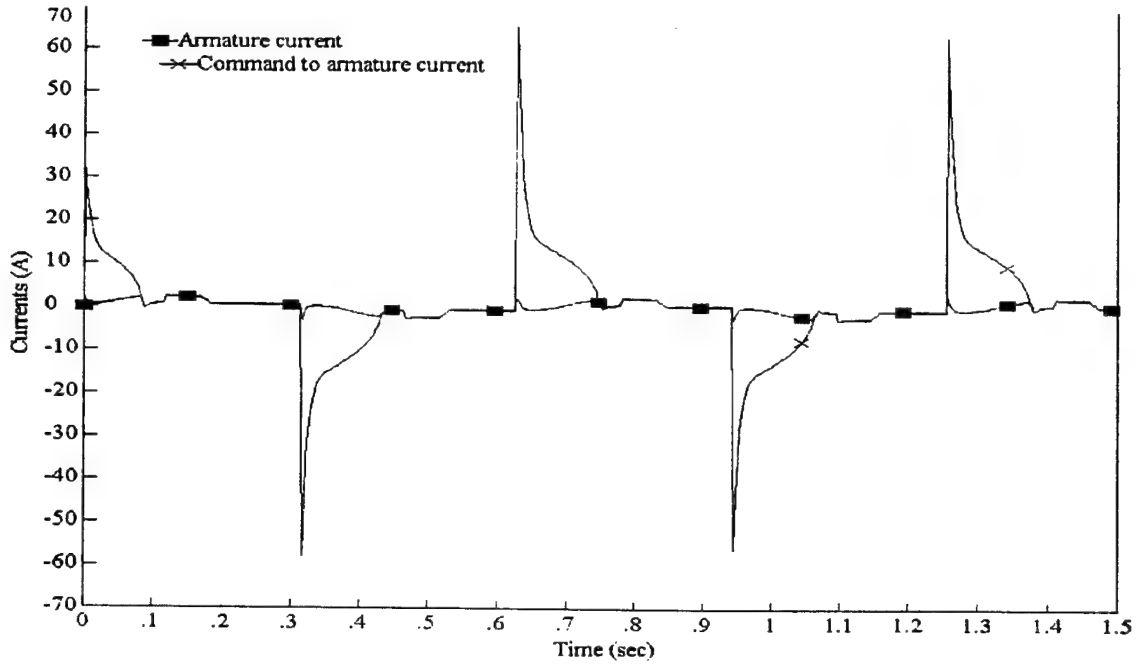

Fig. 4 Current i_a and current command i_{ac} ($\theta_{Lc} = 0.2 sign(\sin t)$)

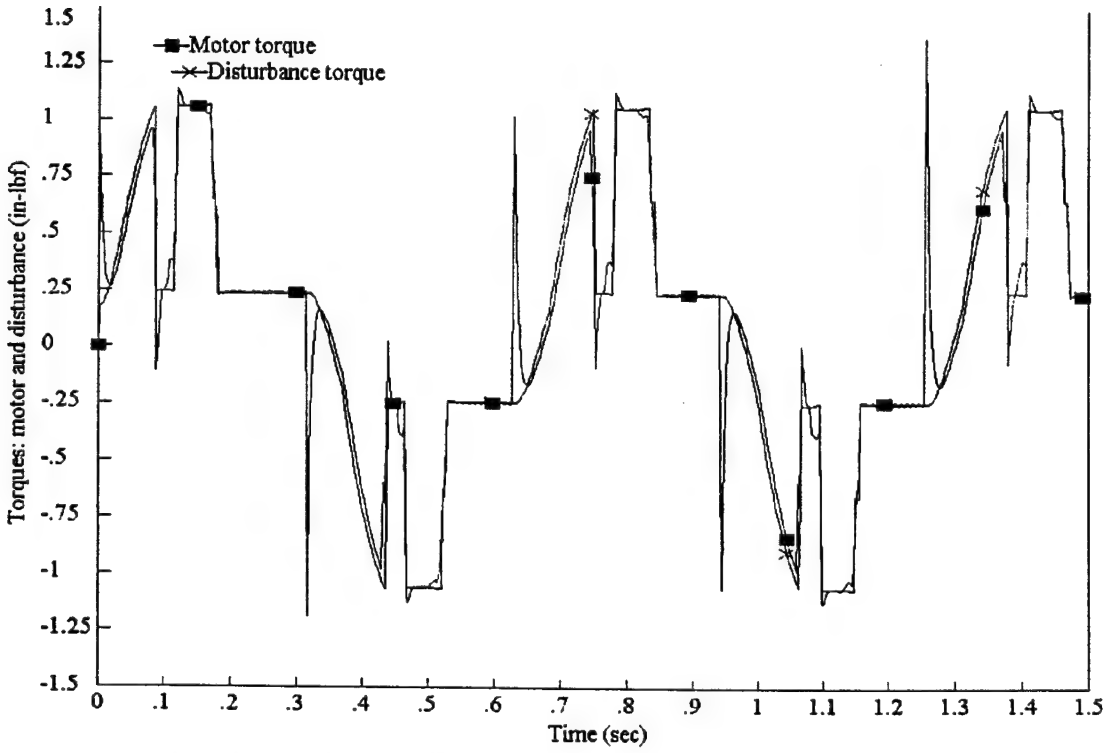

Fig. 5 Torques: motor torque and disturbance torque ($\theta_{Lc} = 0.2 sign(\sin t)$)

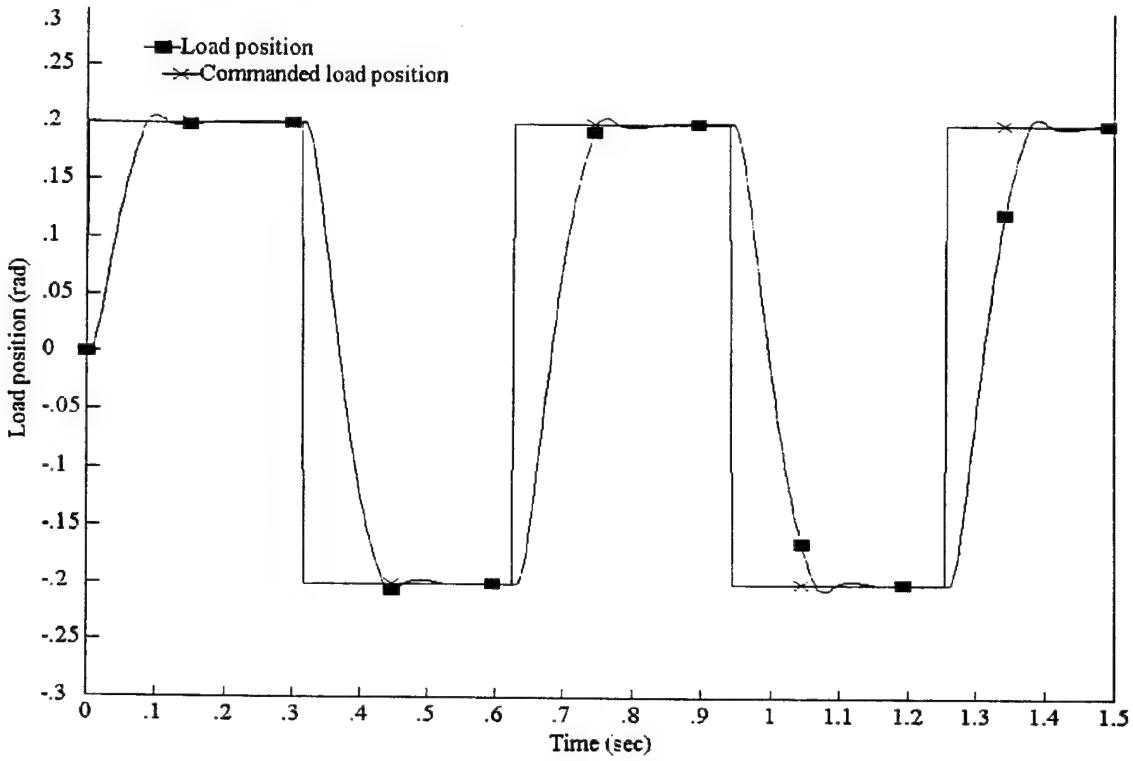

Fig. 6 Load position tracking ($\theta_{Lc} = 0.2 sign(\sin t)$)

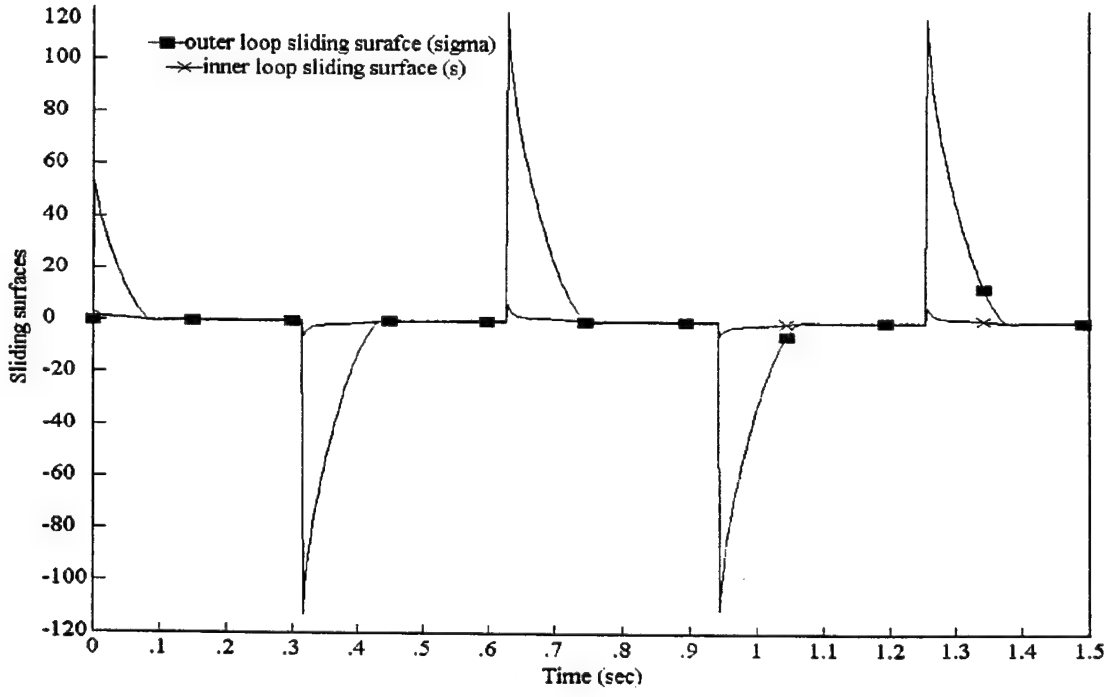

Fig. 7 Sliding surfaces ($\theta_{Lc} = 0.2 sign(\sin t)$)

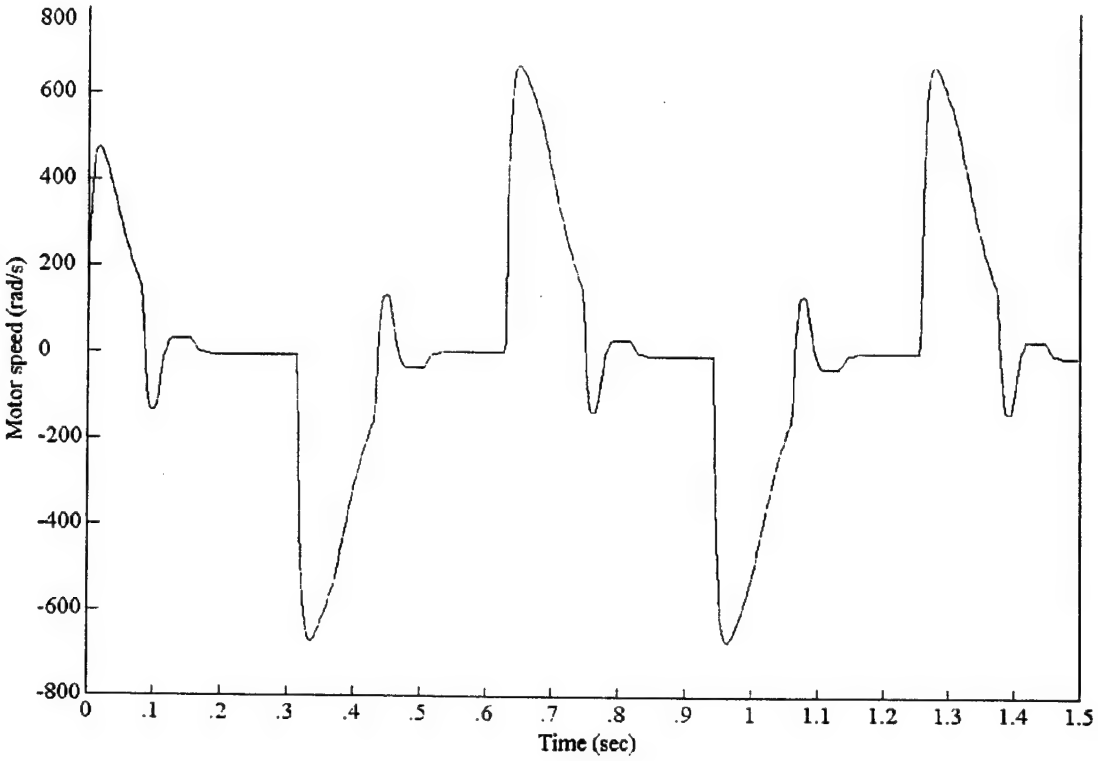

Fig. 8 Motor speed ($\theta_{Lc} = 0.2sign(\sin t)$)

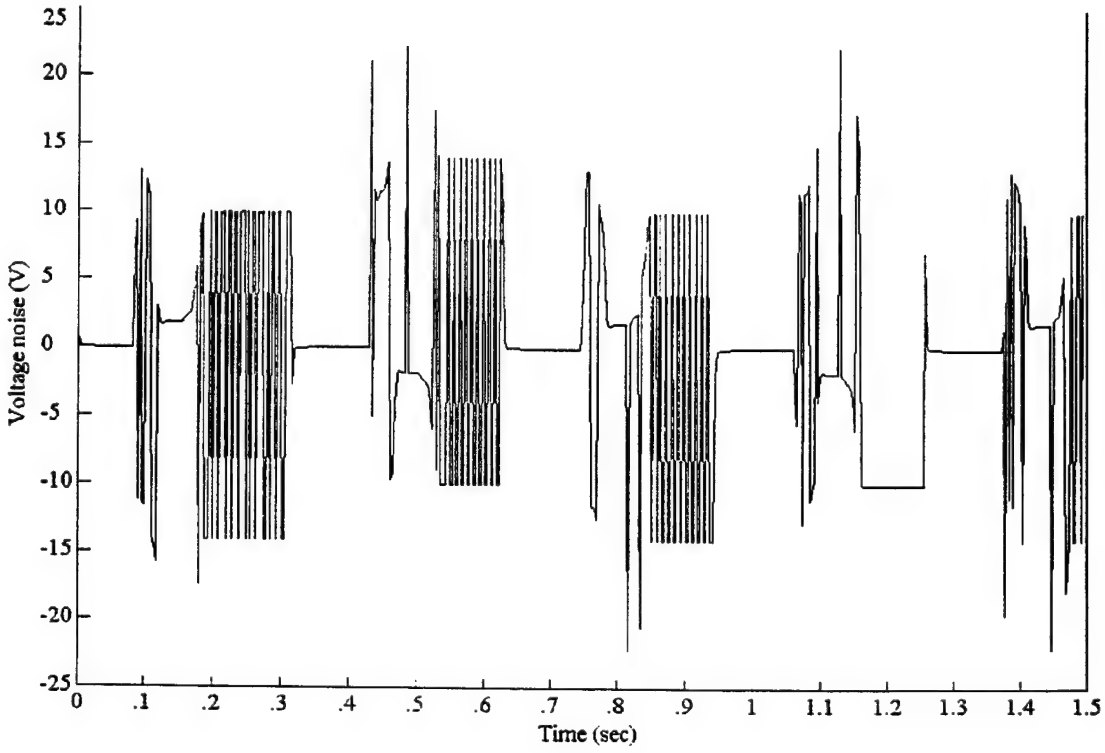

Fig. 9 Voltage noise ($\theta_{Lc} = 0.2sign(\sin t)$)

Analyzing simulation results we can say that control voltage v_a is a high frequency switching function (fig. 3) even without any special efforts such as PWM. Sliding mode holds on time intervals where sliding surfaces are close to zero (fig. 7). Armature current accurately follows armature current command on time intervals when sliding mode holds (fig. 4). Load position command is tracked well (fig. 6). It is observed that due aggressive load position profiles (step function) sliding mode is destroyed on relatively large time intervals where the control system acts as open loop. No effect of voltage noise (fig. 9) to load position tracking is observed.

The second set of simulations was performed for $\theta_{Lc} = 0.2\sin t$. The results of simulations are shown in figures 10-16.

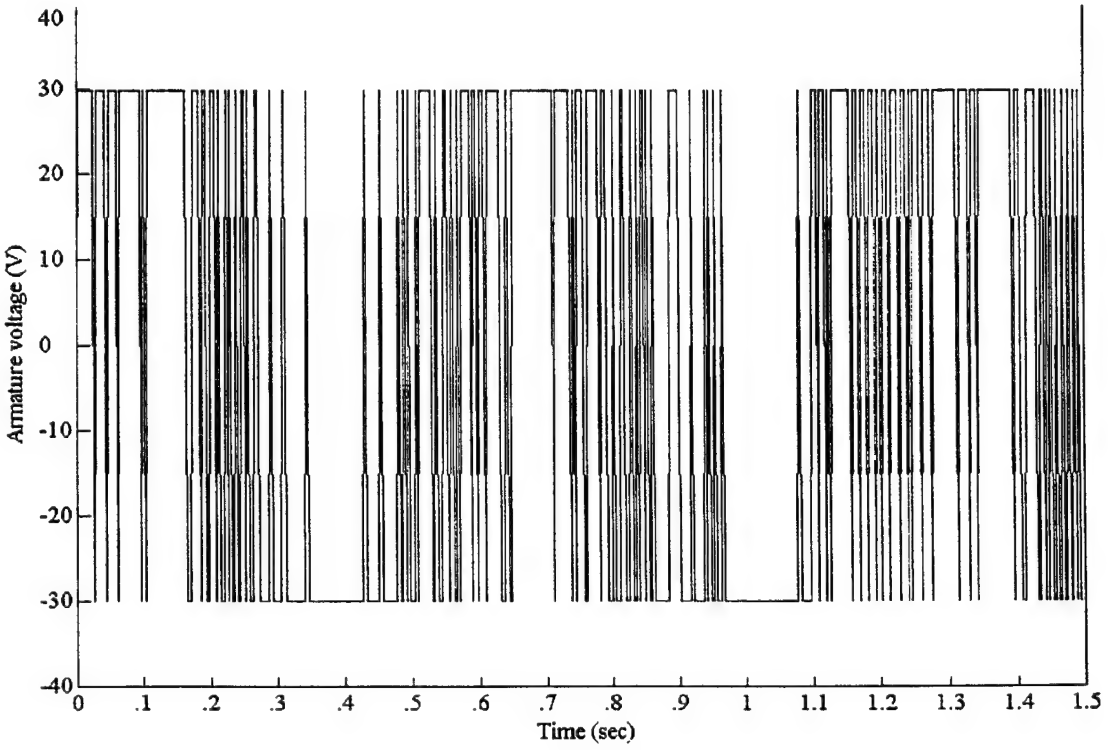

Fig.10 Armature voltage v_a ($\theta_{Lc} = 0.2\sin t$)

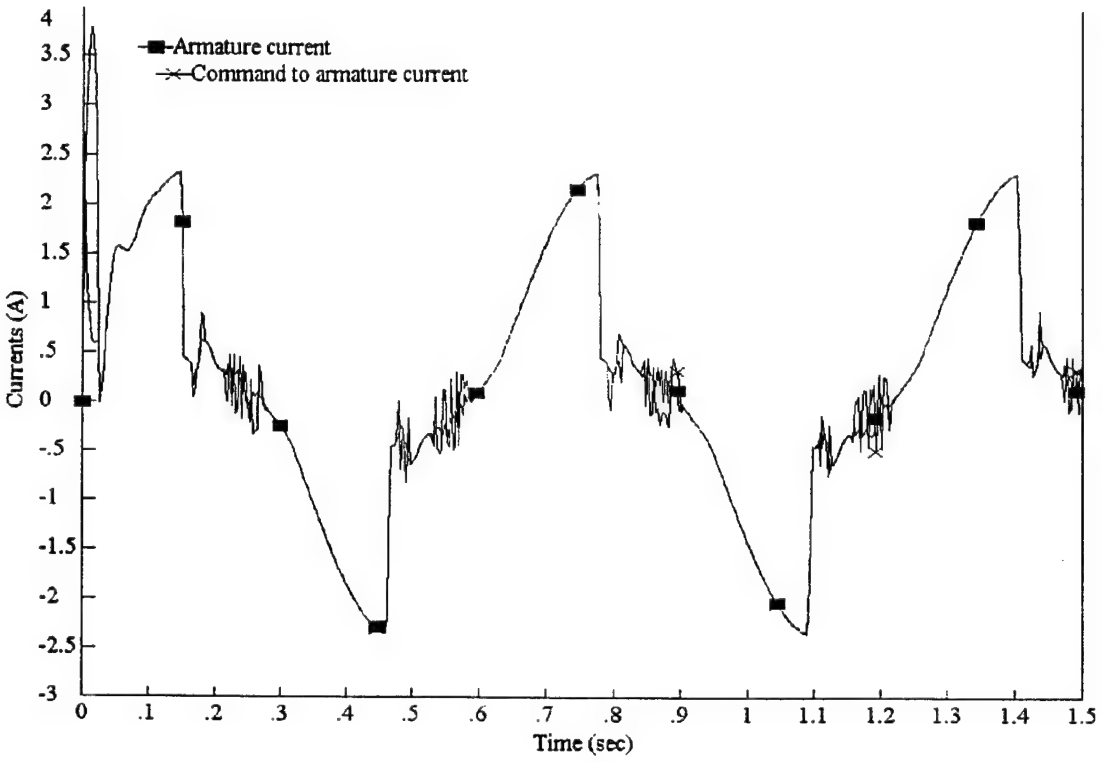

Fig. 11 Current i_a and current command i_{ac} ($\theta_{Lc} = 0.2\sin t$)

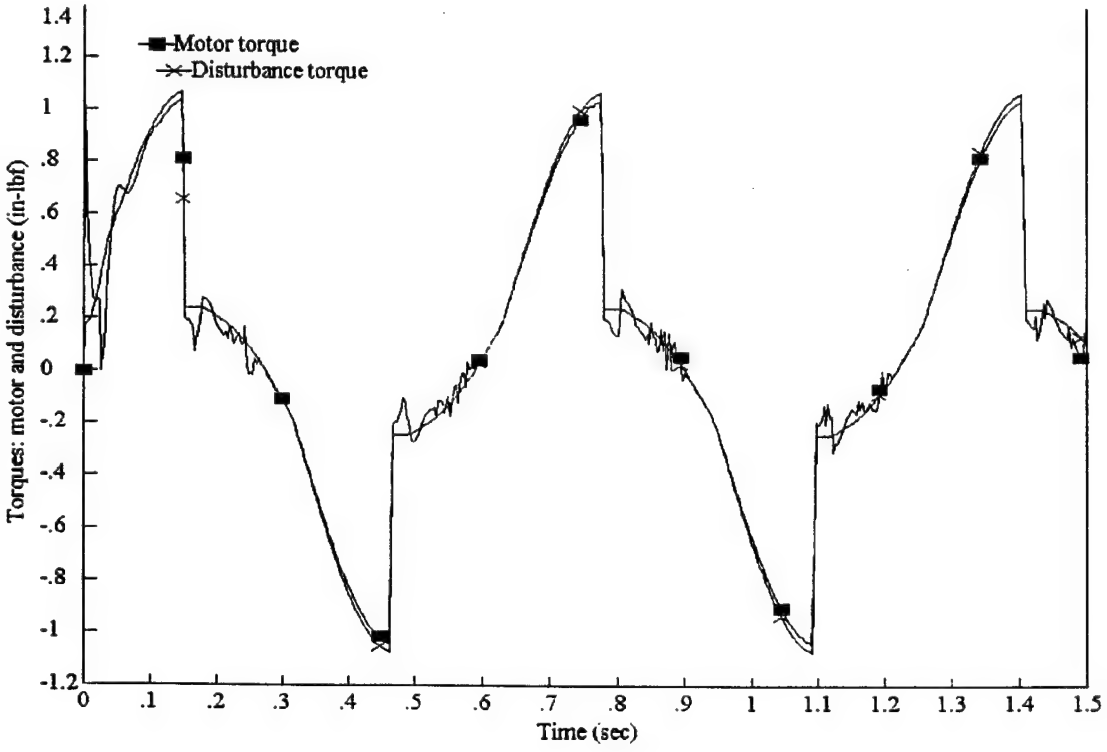

Fig. 12 Torques: motor torque and disturbance torque ($\theta_{Lc} = 0.2\sin t$)

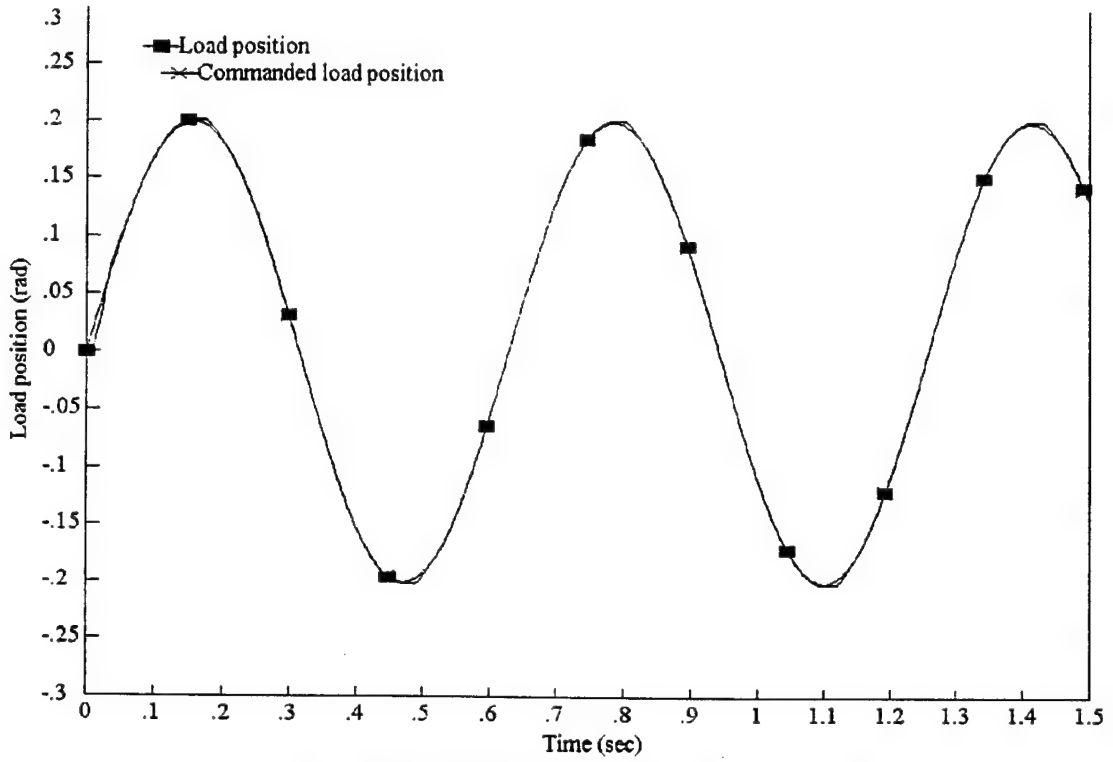

Fig. 13 Load position tracking ($\theta_{Lc} = 0.2\sin t$)

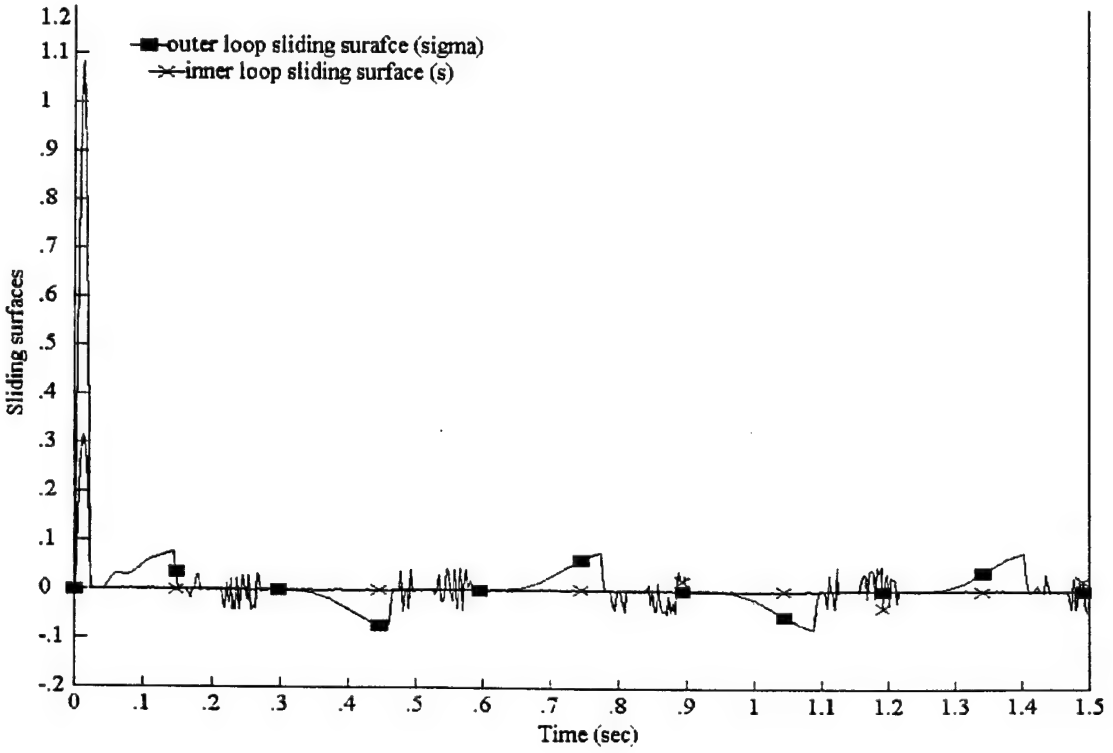

Fig. 14 Sliding surfaces ($\theta_{Lc} = 0.2\sin t$)

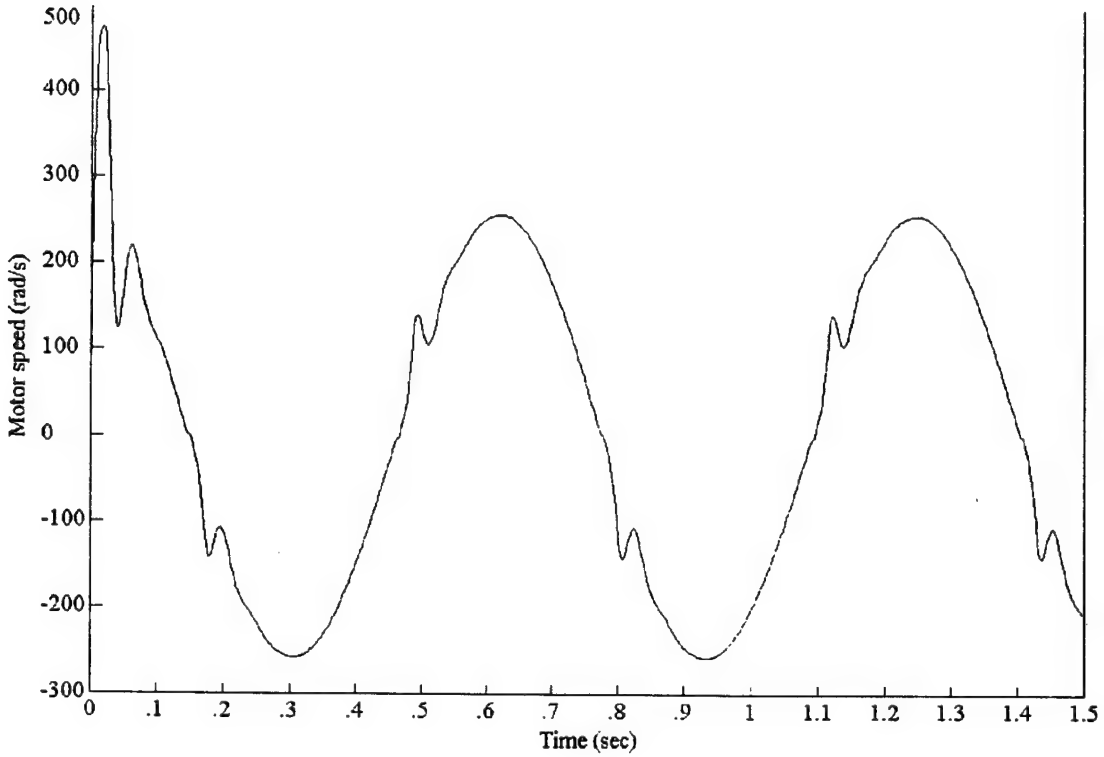

Fig. 15 Motor speed ($\theta_{Lc} = 0.2\sin t$)

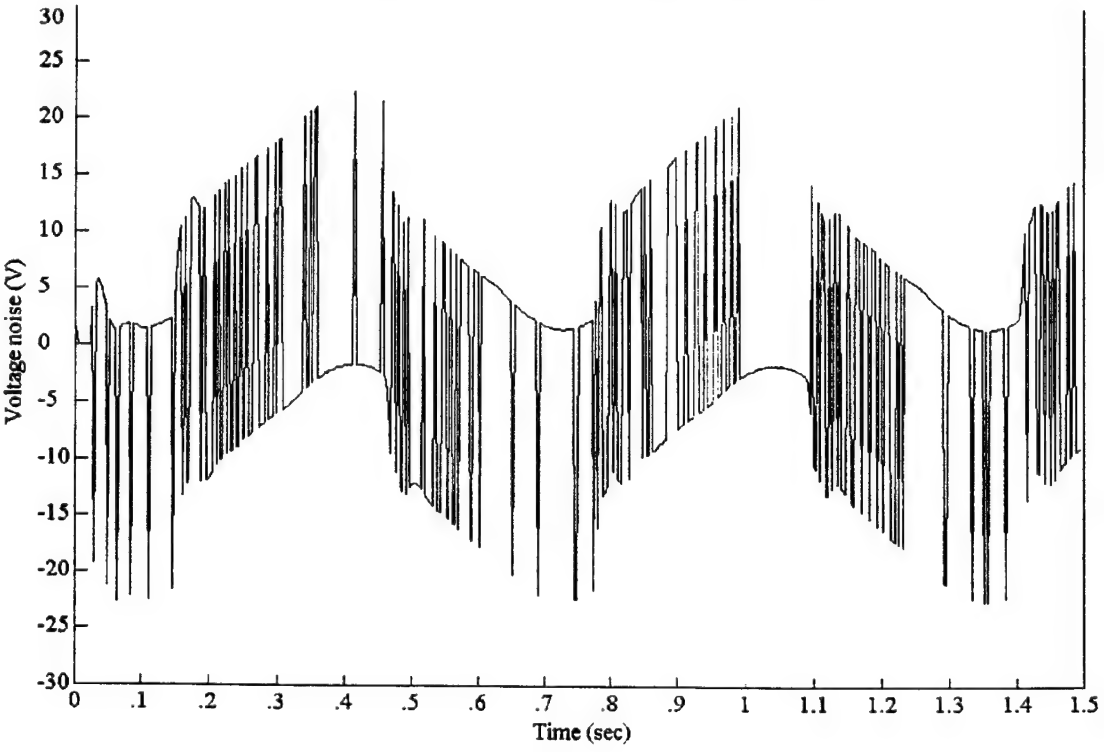

Fig. 16 Voltage noise ($\theta_{Lc} = 0.2\sin t$)

Analyzing simulation results we can say that again control voltage v_a is a high frequency switching function (fig. 10) without any special efforts such as PWM. Sliding mode holds on time intervals where sliding surfaces are close to zero (fig. 14). It is important that sliding mode holds almost all over the control interval. Armature current accurately follows armature current command (fig. 11). Load position command is tracked very accurately (fig. 13). No effect of voltage noise (fig. 16) to load position tracking is observed.

Simulations were repeated with inner loop SMC implemented in a PWM format. Dither signal $\varphi(t)$ was in a triangle periodical format with period equal to 0.0001 s. Amplitude of a dither signal was equal to 0.5. The inner loop SMC was implemented as follows:

$$v_a = 31\, sign\, \tilde{s}\,, \qquad \tilde{s} = s + \varphi(t)\,. \tag{104}$$

The results of the simulations were pretty much the same. I have an impression that the voltage noise does not significantly affect frequency of control switching, because it has the same frequency as the armature voltage v_a. However, the switching frequency of the armature voltage v_a looks somewhat higher with PWM implementation comparing with relay implementation of the SMC. It doesn't hurt to use PWM implementation of the SMC. And, of course, it makes sense to implement the inner loop SMC in a PWM format to protect the controller switching frequency from other noises. Amplitude of a dither signal must be greater then amplitude of summarized noise containing in the sliding surface equation (96).

8. Single loop SMC design (method of system center).

Employing the method of system center (chapter 4) we rewrite the mathematical model of the servomechanism (1) in errors. This is

$$\begin{cases} \dfrac{d\tilde{\theta}_L}{dt} = 0.00794\tilde{\omega}_m + \left[\dot{\theta}_{Lc} - 0.00794\omega_{mc}\right] \\ \dfrac{d\tilde{\omega}_m}{dt} = 35039\tilde{i}_a + \left[\dot{\omega}_{mc} - 35039 i_{ac} + 78740F(.)\right] \\ \dfrac{d\tilde{i}_a}{dt} = 277.8\left(-v_a - 10.0\tilde{i}_a - 0.0503\tilde{\omega}_m\right) + \left[\dot{i}_{ac} + 2778 i_{ac} + 14.0\omega_{mc} - 277.8 n_v\right] \\ \tilde{y} = \tilde{\theta}_L + \left[y_c - \theta_{Lc}\right] \end{cases} \tag{105}$$

where

ω_{mc}, i_{ac} are command signals for ω_m, i_a,

$\tilde{\theta}_L = \theta_{Lc} - \theta_L$, $\tilde{\omega}_m = \omega_{mc} - \omega_m$, $\tilde{i}_a = i_{ac} - i_a$ are state variable tracking errors.

Assuming the load position reference profile $\theta_{Lc}(t)$ is given in real time, the problem is to design a SMC $v_a(t)$ achieving an asymptotic tracking

$$\lim_{t\to\infty}\left|\tilde{\theta}_L(t)\right| = 0. \tag{106}$$

The command profiles i_{ac} and ω_{mc} must be identified through solution of equations of the system center (22) given load position reference (command) profile $y_c = \theta_{Lc}$. This is

$$\omega_{mc} = 125.9\dot{\theta}_{Lc}, \quad i_{ac} = 0.00359\ddot{\theta}_{Lc} + 2.247F(.). \tag{107}$$

Having state variable profiles i_{ac} and ω_{mc} given in real time, the output tracking problem (105), (106) can be transformed to the following state variable tracking problem:

$$\begin{cases} \dfrac{d\tilde{\theta}_L}{dt} = 0.00794\tilde{\omega}_m \\ \dfrac{d\tilde{\omega}_m}{dt} = 35039\tilde{i}_a \\ \dfrac{d\tilde{i}_a}{dt} = 277.8\left(-v_a - 10.0\tilde{i}_a - 0.0503\tilde{\omega}_m\right) + \Phi(.) \\ \tilde{y} = \tilde{\theta}_L \end{cases} \tag{108}$$

$$\lim_{t\to\infty}|\tilde{\theta}_L(t)| = \lim_{t\to\infty}|\tilde{i}_a(t)| = \lim_{t\to\infty}|\omega_m(t)| = 0, \tag{109}$$

where $\Phi(.) = 0.00359\ddot{\theta}_{Lc} + 9.72\ddot{\theta}_{Lc} + 1762.6\dot{\theta}_{Lc} + 2.247\dot{F}(.) + 6242.2F(.) - 277.8n_v$.

8.1 Sliding surface design

At the first step of the outer loop SMC design the sliding surface is identified as follows:

$$s = \tilde{i}_a + c_1\tilde{\omega}_m + c_2\tilde{\theta}_L = 0. \tag{110}$$

In order to identify parameters c_1 and c_2 of the sliding surface (110) the system's (108) motion on the sliding surface (110) is derived. This is

$$\begin{cases} \dfrac{d\tilde{\theta}_L}{dt} = 0.00794\tilde{\omega}_m \\ \dfrac{d\tilde{\omega}_m}{dt} = -35039(c_1\tilde{\omega}_m + c_2\tilde{\theta}_L). \\ \tilde{y} = \tilde{\theta}_L \end{cases} \tag{111}$$

Requiring the desired characteristic equation

$$(\lambda + 500)^2 = \lambda^2 + 1000\lambda + 250000 = 0, \tag{112}$$

the corresponding values of parameters c_1 and c_2 were identified

$$c_1 = 0.029, \quad c_2 = 899. \tag{113}$$

8.2 SMC design

At the second step the SMC law v_a is designed to asymptotically stabilize $s = 0$. The sliding surface dynamics are described as follows:

$$\dot{s} = -277.8v_a - 1762\tilde{i}_a - 6.87\tilde{\omega}_m + \Phi(.). \tag{114}$$

Equivalent control that provides the system's motion on the sliding surface is identified nullifying a derivative of the sliding surface (114). This is

$$v_{aeq} = -6.34\tilde{i}_a - 0.025\tilde{\omega}_m + 0.0036\Phi(.). \tag{115}$$

The SMC is identified in the format (100) as follows:

$$v_a = \rho \, sign \, s, \tag{116}$$

where $\rho > |v_{aeq}|$, or in the other words

$$\rho > \left|-6.34\tilde{i}_a - 0.025\tilde{\omega}_m + 0.0036\Phi(.)\right|. \tag{117}$$

In accordance to physical limitation to the armature voltage the SMC (116) is chosen as follows:

$$v_a = 31 \, sign \, s. \tag{118}$$

Inequality (117) becomes

$$\left|-6.34\tilde{i}_a - 0.025\tilde{\omega}_m + 0.0036\Phi(.)\right| < 31 \tag{119}$$

and gives a domain of existence of sliding mode on the surface (110), (113).

8.3 Disturbance observation

Implementing the SMC (110), (113), (118) we have to calculate state variable commanded profiles i_{ac} and ω_{mc} (107). These profiles contain the disturbance $F(.)$, which can be calculated (fig. 2) or estimated, in case when it is not known exactly. The sliding mode observer [10] was designed to estimate the disturbance $F(.)$. Designing the sliding mode observer we used the second equation from servomechanism mathematical model

$$\frac{d\omega_m}{dt} = 78740\left(0.445 i_a - F(.)\right). \tag{120}$$

Assuming i_a measuring accessible we estimate $\dot{\omega}_m$ as follows [10]:

$$\begin{cases} \dot{\hat{\omega}}_m = -Ksign(\hat{\omega}_m - \omega_m) \\ \tau\dot{z} = -z - Ksign(\hat{\omega}_m - \omega_m), \\ \hat{\omega}_m = z \end{cases} \tag{121}$$

and the disturbance $F(.)$ is estimated as follows:

$$\hat{F}(.) = 0.445 i_a - 0.0000127 z. \tag{122}$$

The sliding mode observer was implemented in a continuous format. This is

$$\begin{cases} \dot{\hat{\omega}}_m = -50000(\hat{\omega}_m - \omega_m) \\ \hat{F}(.) = 0.445 i_a + 0.635(\hat{\omega}_m - \omega_m) \end{cases} \tag{123}$$

8.4 Simulation of the servomechanism with a single loop SMC

The system (1) was simulated with the single loop SMC (110), (113), (118) implemented in a PWM format (104). Nonlinearities were taken into account. Backlash characteristic of the gear train was used with 0.75 width, and the deadband block was used with the deadband equal to 3.0 (fig. 1). The first set of simulations was performed for $\theta_{Lc} = 0.2 sign(\sin t)$. The results of simulations are shown in figures 17-23. Modeling the noise voltage n_v we assume that armature current discontinuity, which is caused by switching control voltage v_a, leads to the noise voltage n_v. During simulation the noise voltage n_v is modeled as follows: $n_v = 4 \cdot 10^{-4} \frac{dv_a}{dt}$. Differentiation is performed numerically.

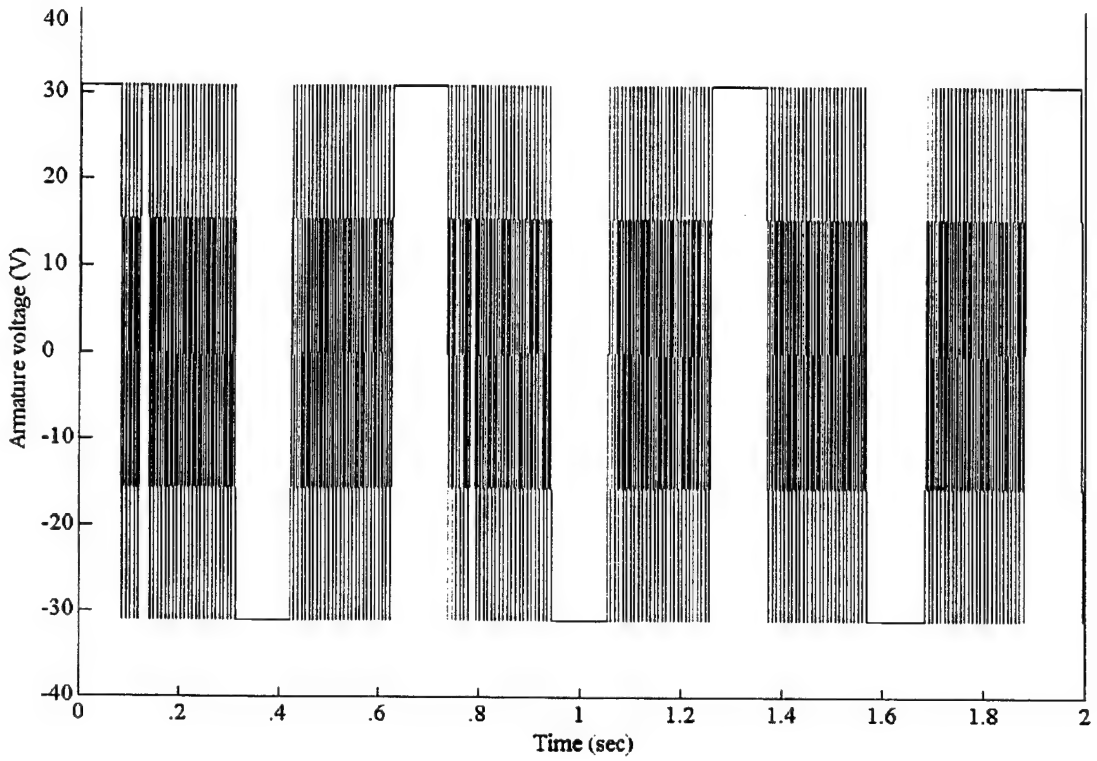

Fig. 17 Armature voltage v_a $(\theta_{Lc} = 0.2sign(\sin t))$

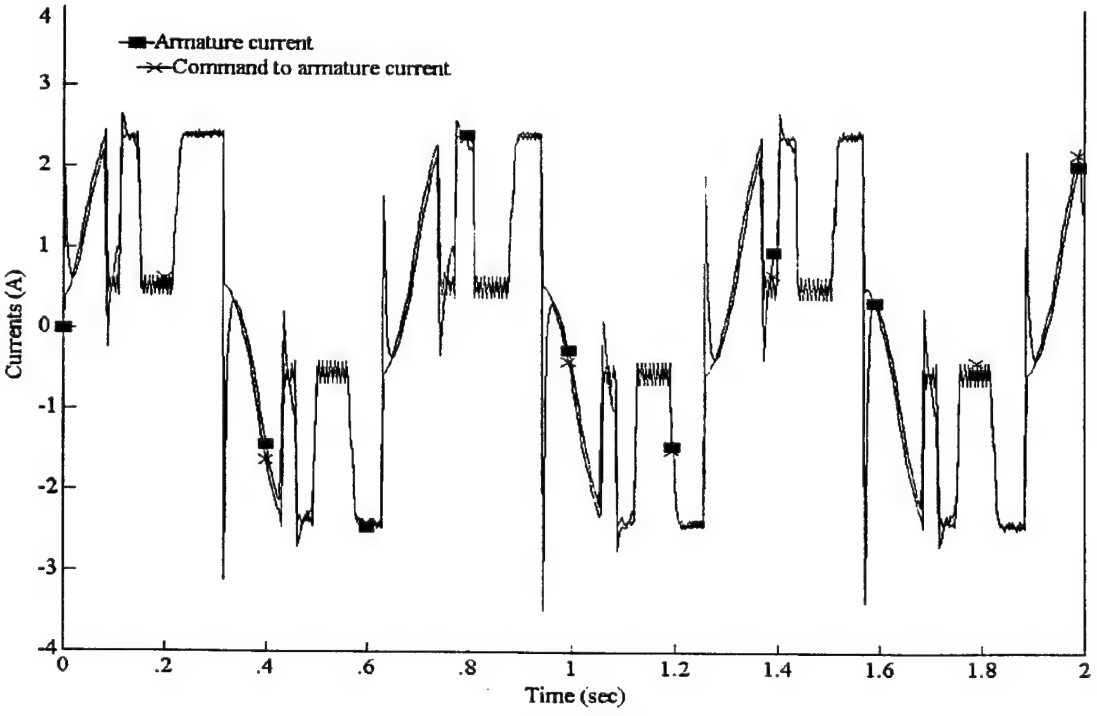

Fig. 18 Current i_a and current command i_{ac} $(\theta_{Lc} = 0.2sign(\sin t))$

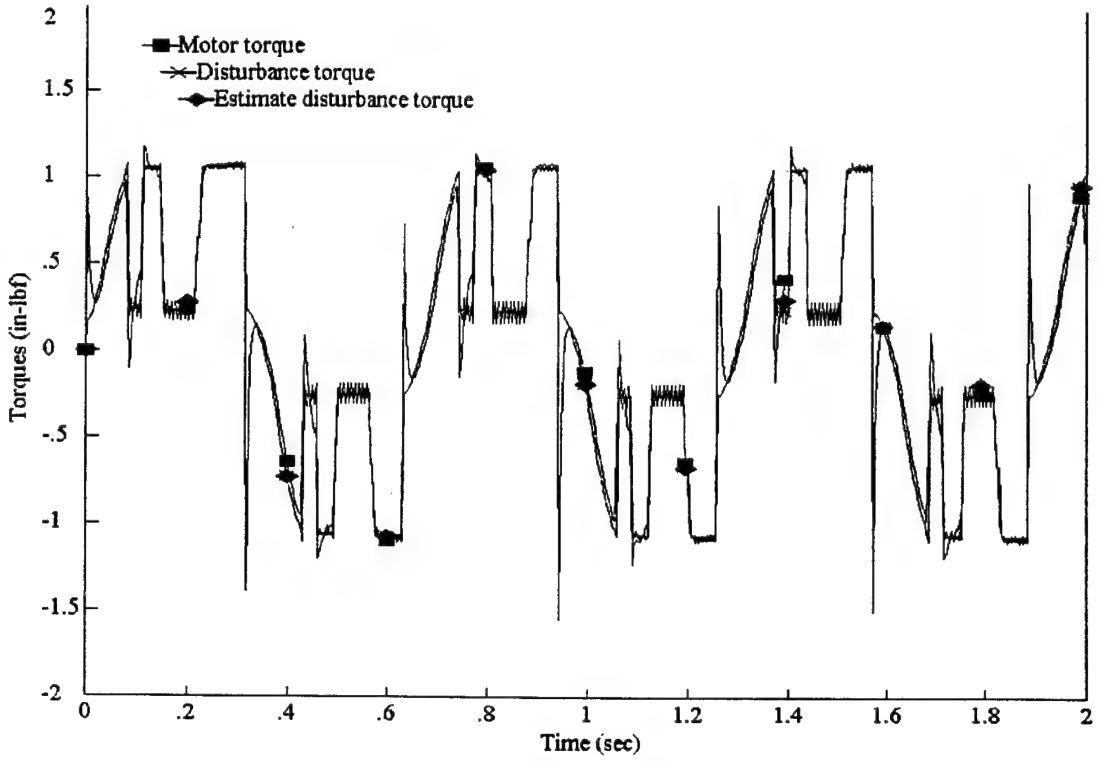

Fig. 19 Torques: motor torque, disturbance torque and estimate ($\theta_{Lc} = 0.2sign(\sin t)$)

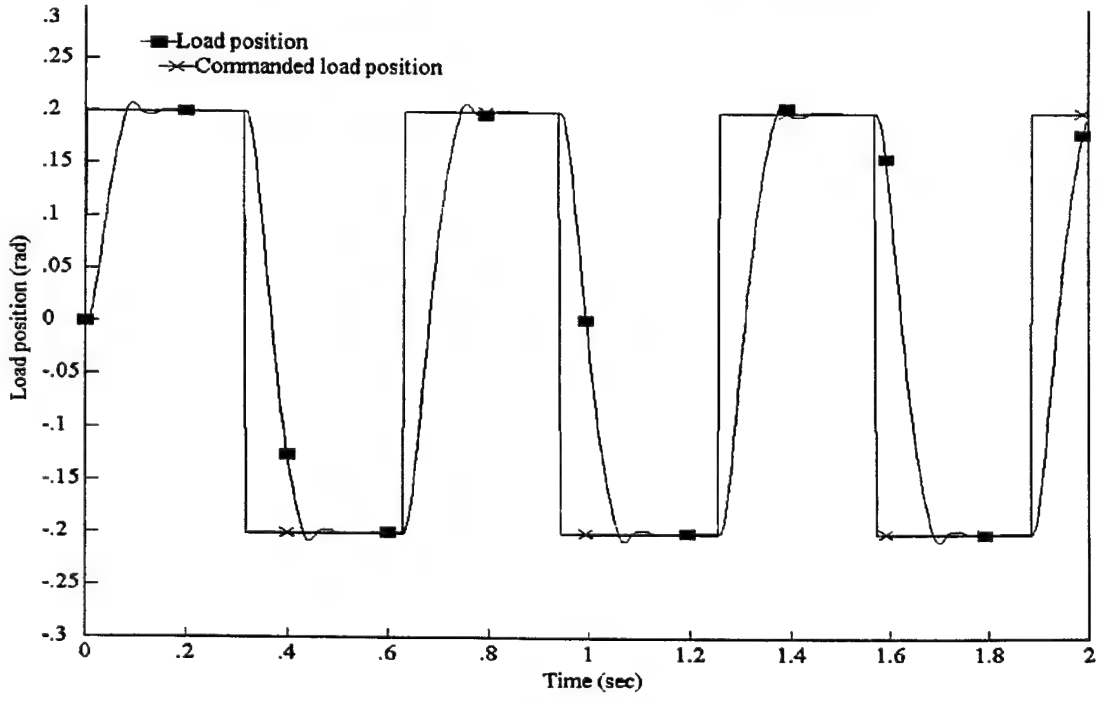

Fig. 20 Load position tracking ($\theta_{Lc} = 0.2sign(\sin t)$)

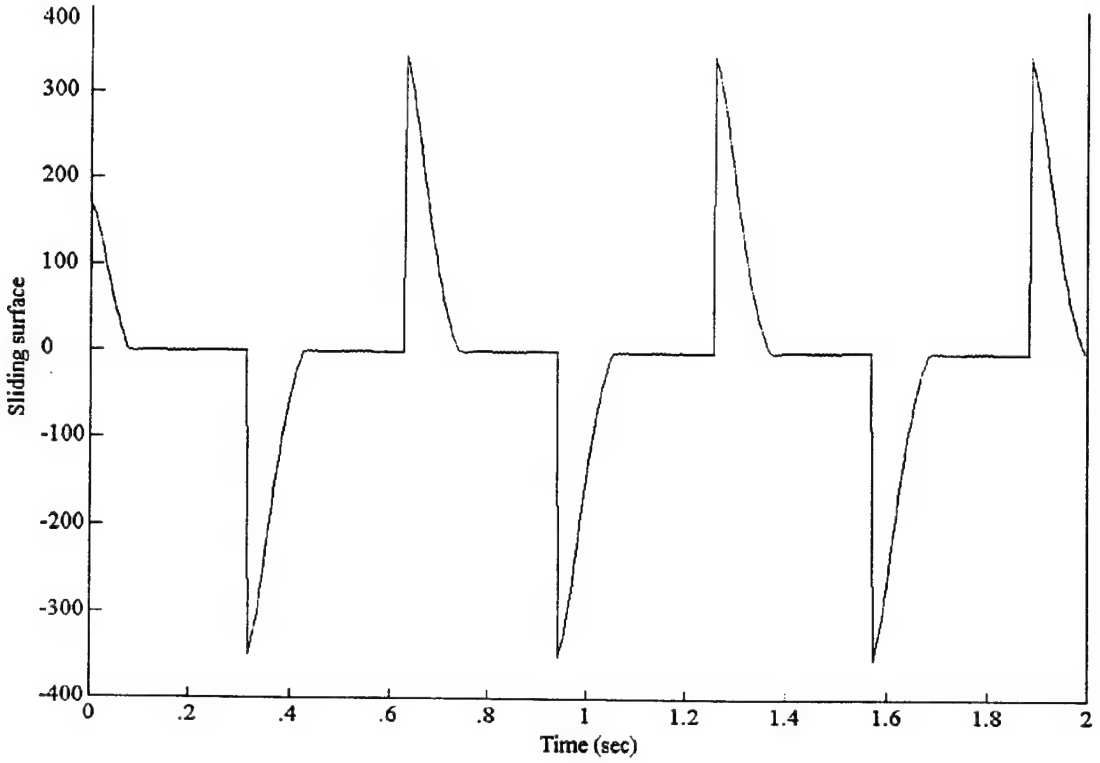

Fig. 21 Sliding surface ($\theta_{Lc} = 0.2 sign(\sin t)$)

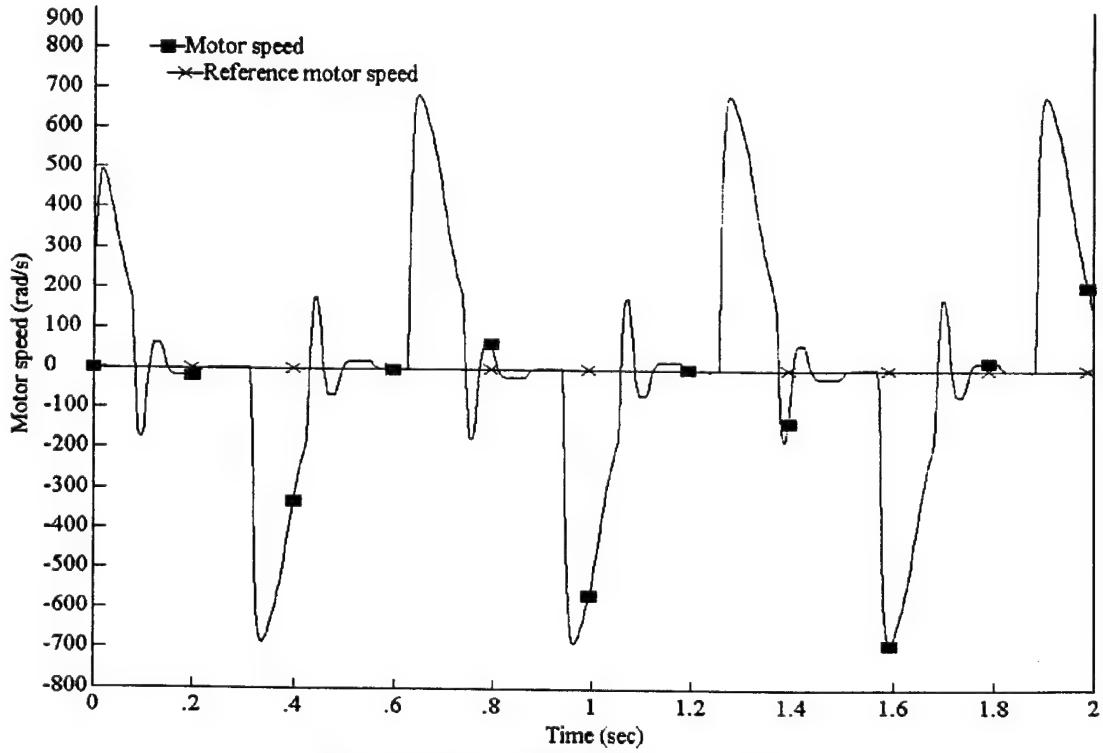

Fig. 22 Motor speed ($\theta_{Lc} = 0.2 sign(\sin t)$)

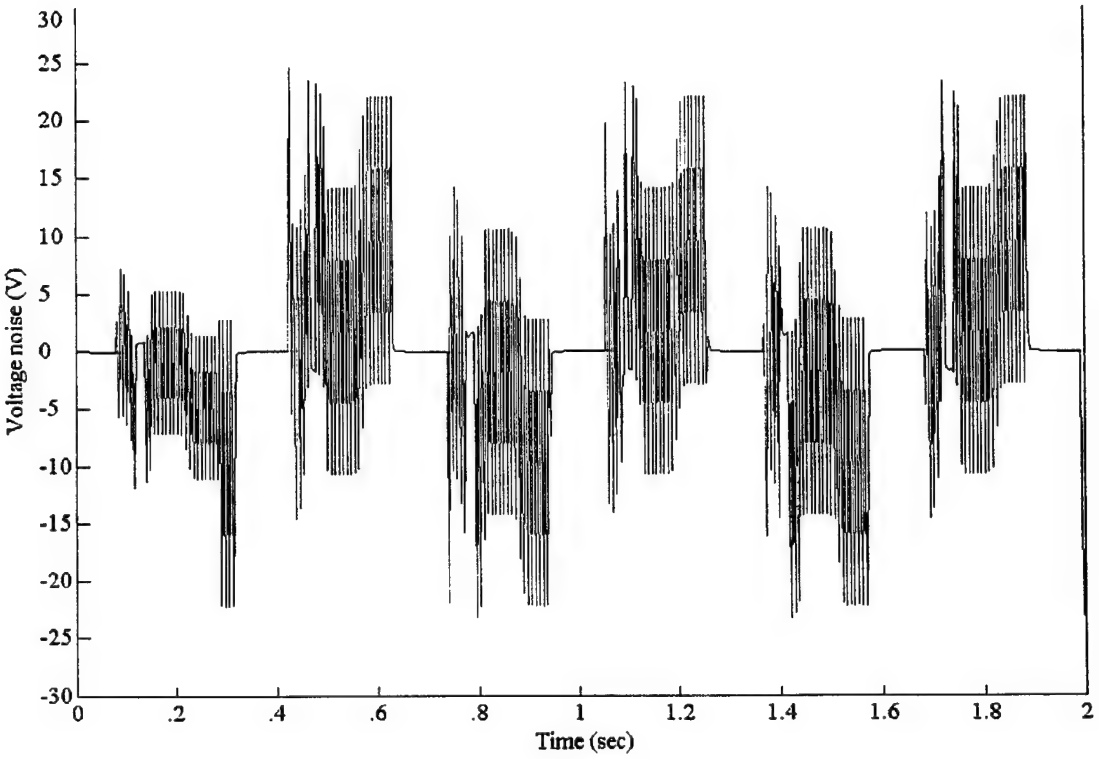

Fig. 23 Voltage noise ($\theta_{Lc} = 0.2 sign(\sin t)$)

Analyzing simulation results we can say that again control voltage v_a is a high frequency switching function (fig. 17). Sliding mode holds on time intervals where sliding surfaces are close to zero (fig. 21). Armature current accurately follows armature current command (fig. 18). Load position command is tracked very accurately (fig.20). No effect of voltage noise (fig. 23) to load position tracking is observed. The system was simulated with the single loop SMC in the relay format (118) as well. The results of the simulations are pretty much the same. However, the switching frequency of the armature voltage v_a looks somewhat higher with PWM implementation comparing with relay implementation of the single loop SMC.

The second set of simulations was performed for $\theta_{Lc} = 0.2 \sin t$ The single loop SMC was implemented in the relay format (118). The results of simulations are shown in figs. 24-30.

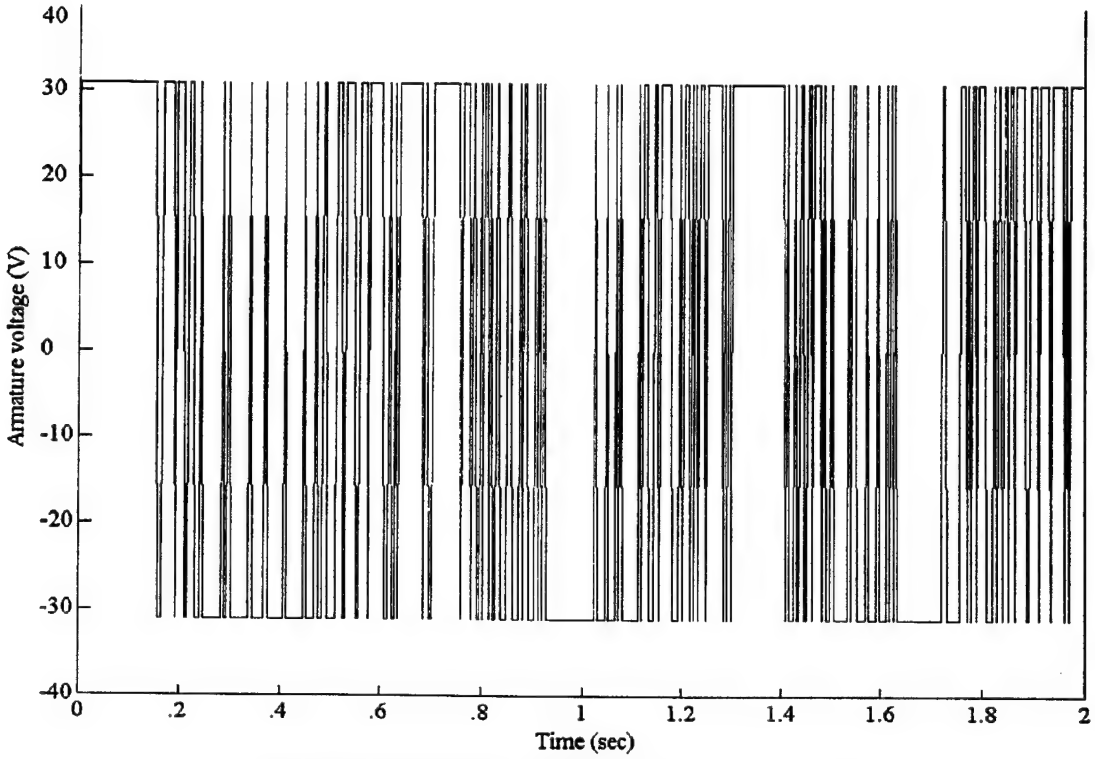

Fig. 24 Armature voltage v_a ($\theta_{Lc} = 0.2\sin t$)

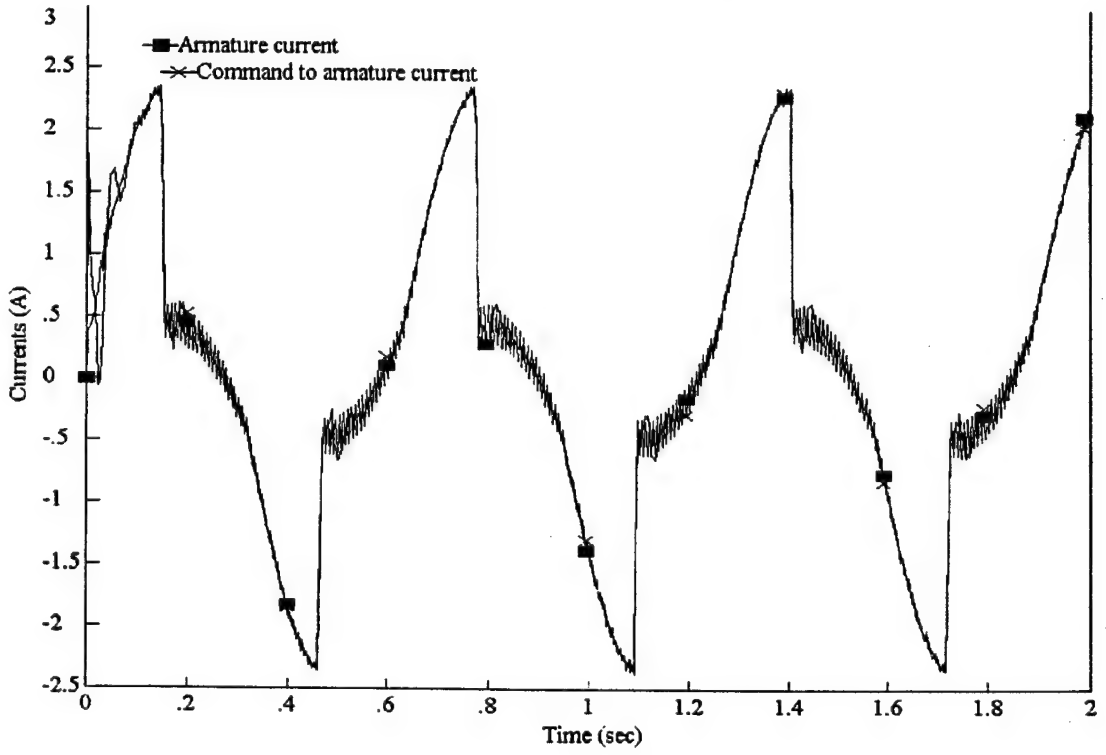

Fig. 25 Current i_a and current command i_{ac} ($\theta_{Lc} = 0.2\sin t$)

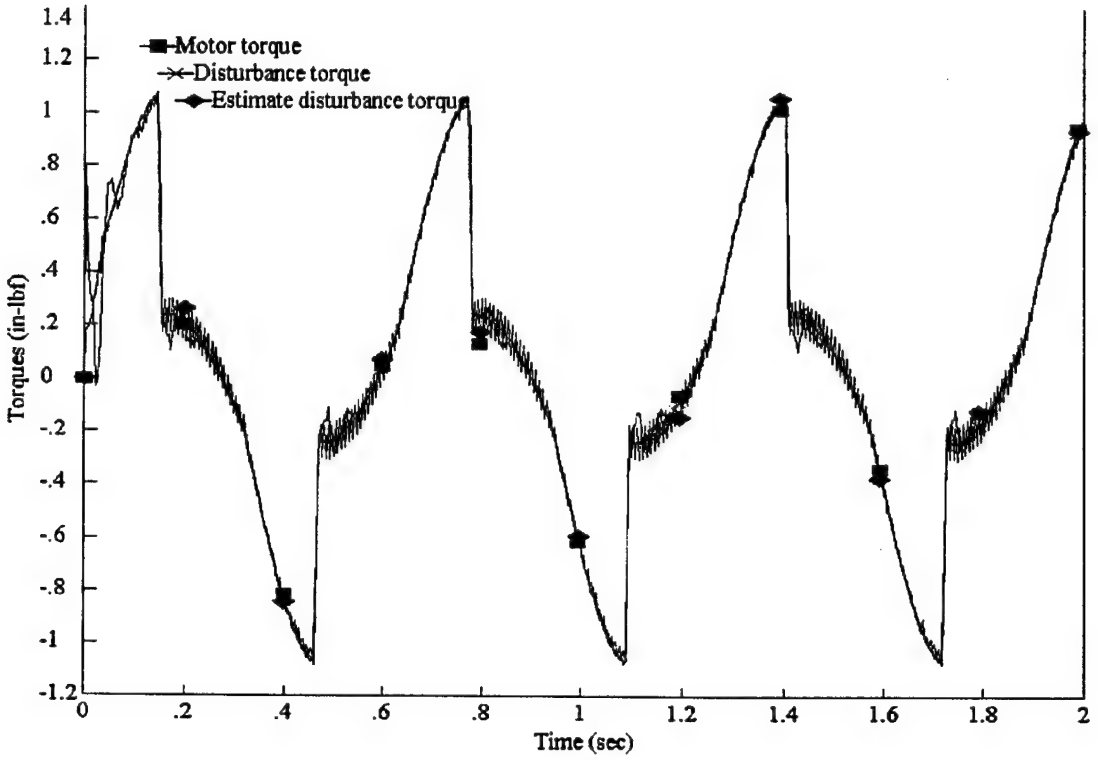

Fig. 26 Torques: motor torque, disturbance torque and estimate ($\theta_{Lc} = 0.2\sin t$)

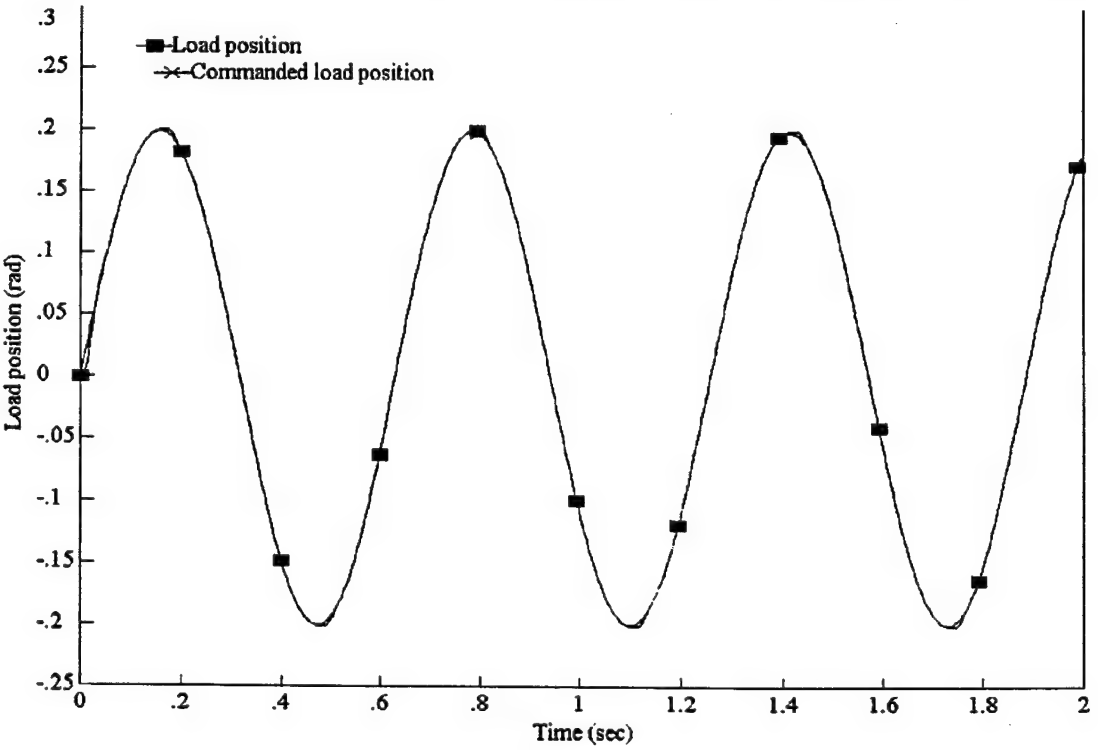

Fig. 27 Load position tracking ($\theta_{Lc} = 0.2\sin t$)

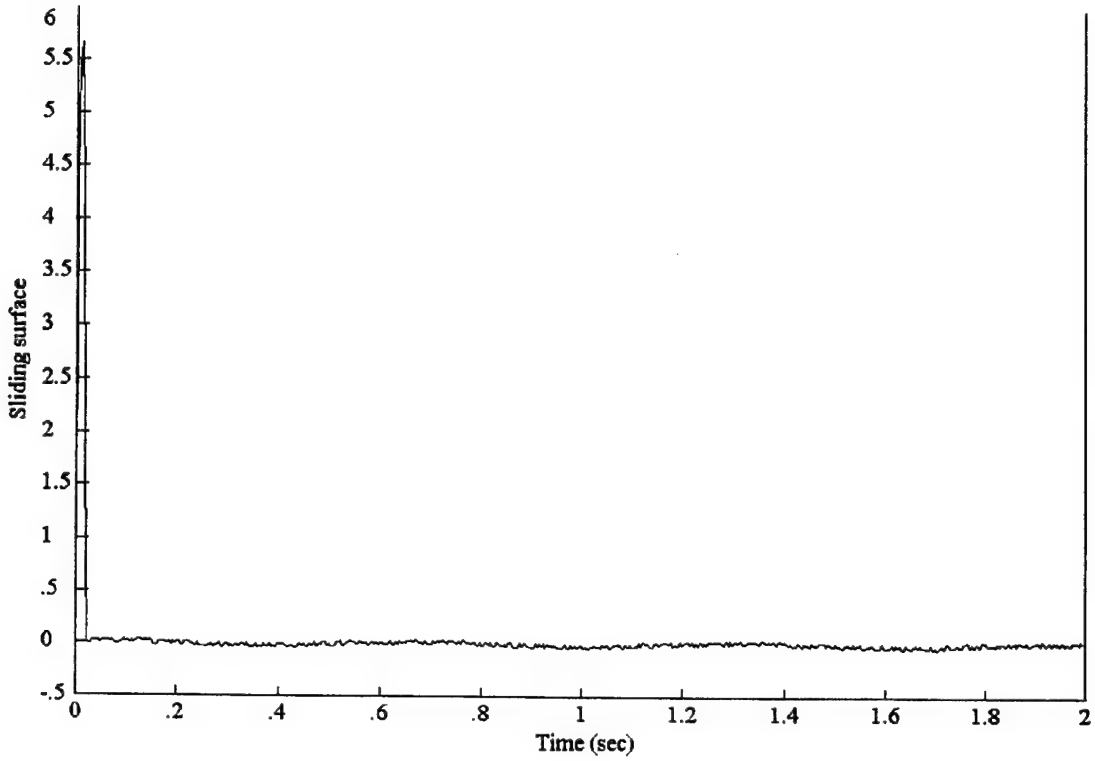

Fig. 28 Sliding surface ($\theta_{Lc} = 0.2\sin t$)

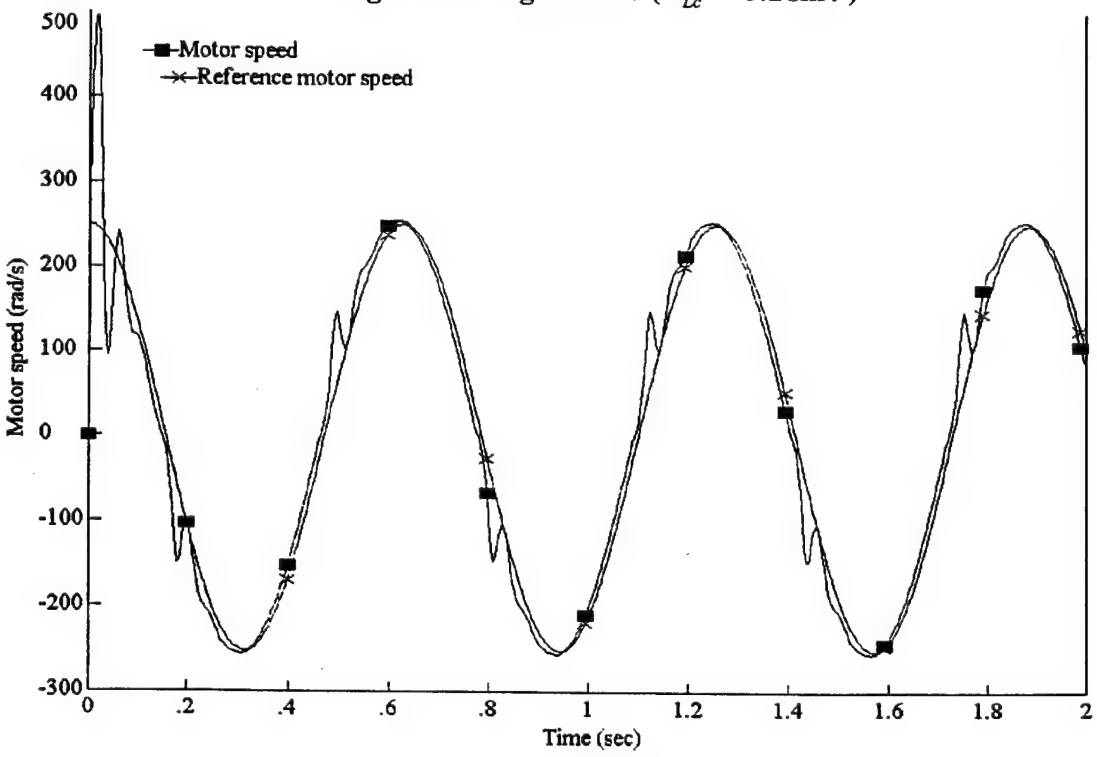

Fig. 29 Motor speed ($\theta_{Lc} = 0.2\sin t$)

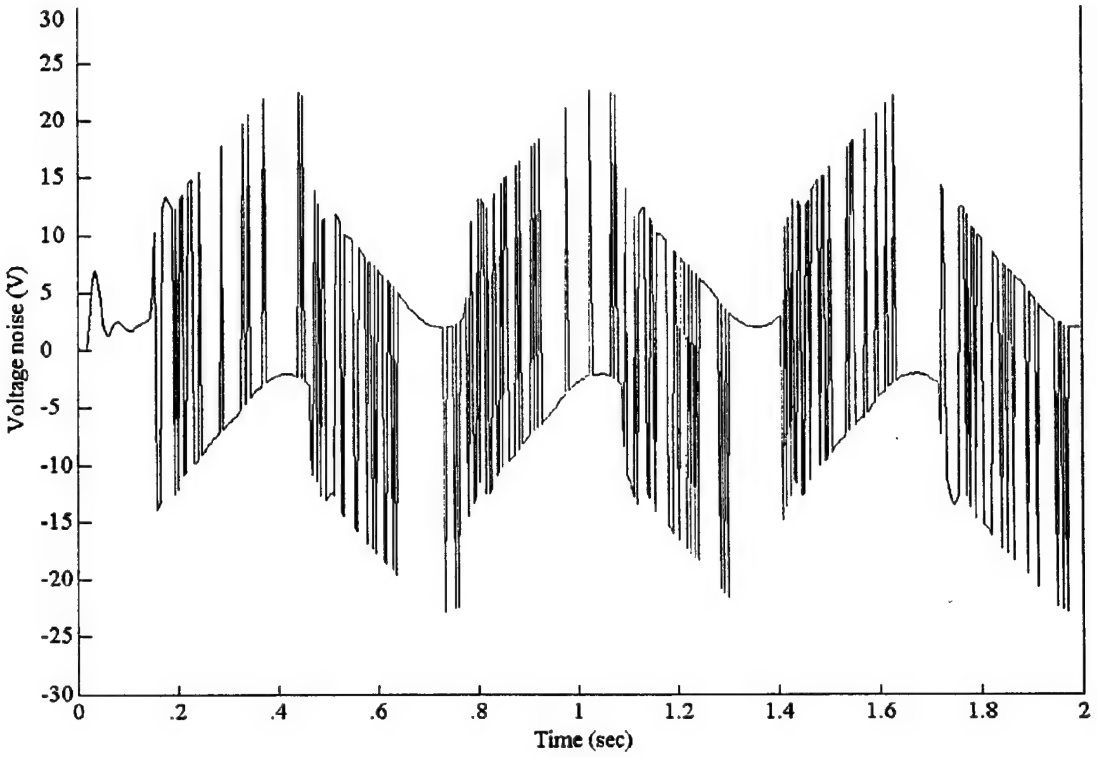

Fig. 30 Voltage noise ($\theta_{Lc} = 0.2\sin t$)

Analyzing simulation results shown in fig. 24 -30 we can say that again control voltage v_a is a high frequency switching function (fig. 24) without any special efforts such as PWM. Sliding mode holds on time intervals where sliding surfaces are close to zero (fig. 28). It is important that sliding mode holds almost all over the control interval. Armature current accurately follows armature current command (fig. 25). Load position command is tracked very accurately (fig. 27). No effect of voltage noise (fig. 30) to load position tracking is observed.

Simulations were repeated with the single loop SMC implemented in a PWM format: $v_a = 31\, sign\, \tilde{s}$, $\tilde{s} = s + \varphi(t)$. Dither signal $\varphi(t)$ was in a triangle periodical format with a period equal to 0.0001 s. Amplitude of a dither signal was equal to 0.5. The dither signal is shown in fig. 31.

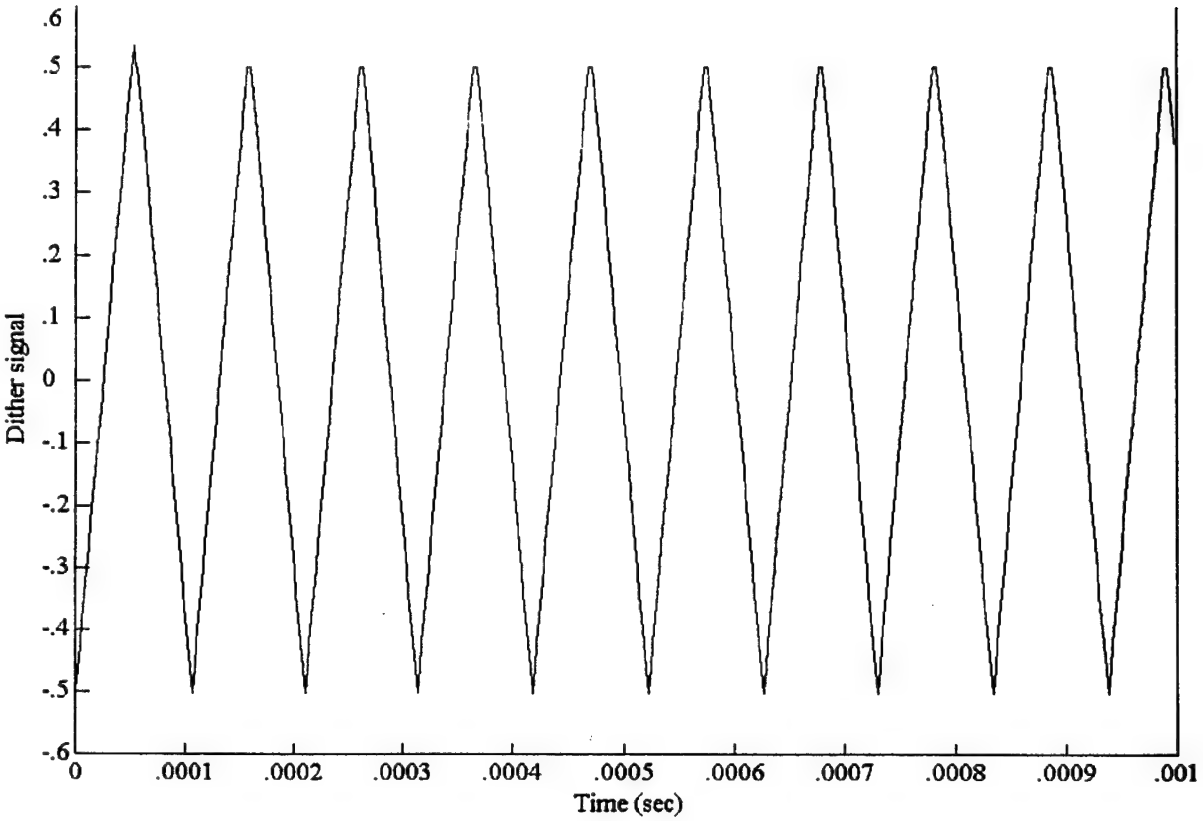

Fig. 31 Dither signal

The results of the simulations were pretty much the same. I have an impression that the voltage noise does not significantly affect frequency of control switching, because it has the same frequency as the armature voltage v_a. However, the switching frequency of the armature voltage v_a (fig. 32) looks somewhat higher with the PWM implementation comparing with the relay implementation of the SMC. Also, it makes sense to implement the inner loop SMC in the PWM format to protect the controller switching frequency from other noises. Amplitude of a dither signal must be greater then amplitude of summarized noise containing in the sliding surface equation. Implementing the inner loop SMC in the PWM format we could include an integration term in a sliding surface equation to compensate for a steady state tracking error.

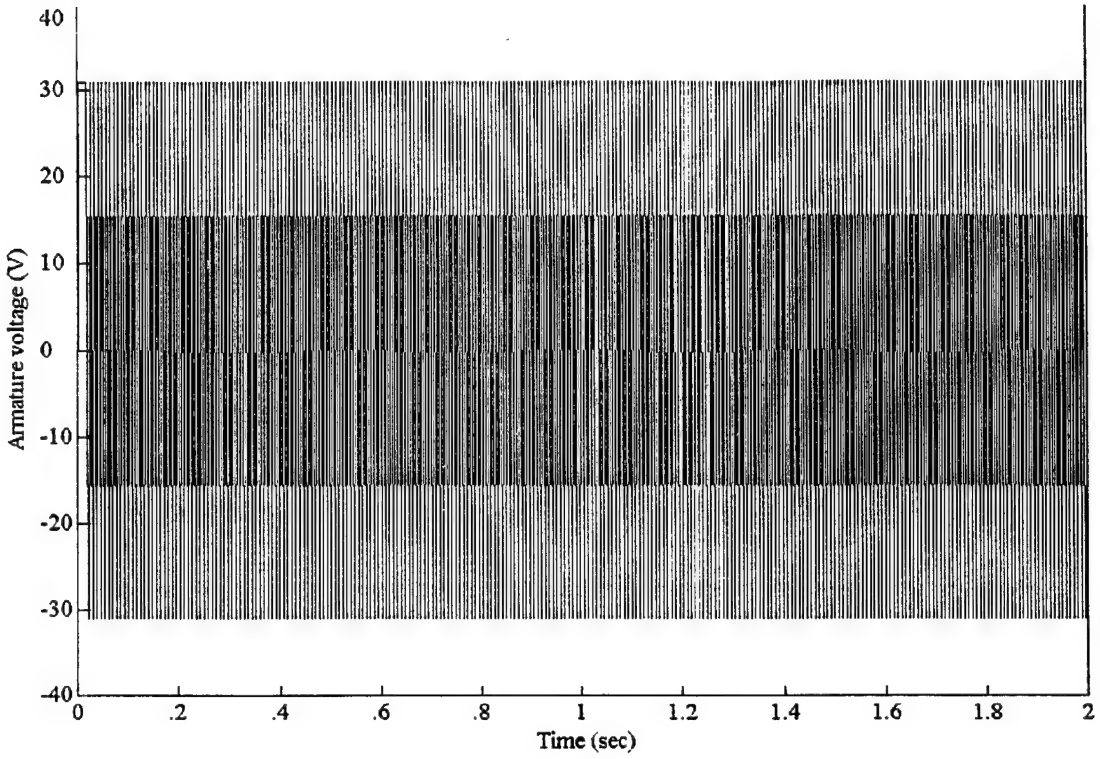

Fig. 32 Armature voltage v_a with PWM ($\theta_{Lc} = 0.2\sin t$)

9. Discrete implementation of the SMC's

Implementing the designed SMC's in a discrete format we take into consideration the following:

1. Command profile $\theta_{Lc}(t)$ has 0.0005s computational delay.
2. Censored load position θ_L, armature current I_a and a motor speed ω_m have 0.001s computational delay.
3. Armature voltage (control function) has 0.001s computational delay.
4. The sliding surfaces s (96) and (110) have 0.0001s sampling-and-holding computational delay.

Both discrete SMC's were simulated in a relay format and PWM format. Nonlinearities were taken into account. Backlash characteristic of the gear train was used with 0.75 width, and the deadband block was used with the deadband equal to 3.0 (fig. 1). It turned out that discrete SMC's implemented in PWM format showed the performance with fewer ripples of armature currents. The system (1) was simulated with the two-loop SMC (87), (93), (96), (100) implemented in a PWM format (104) for $\theta_{Lc} = 0.2sign(\sin t)$. A dither signal (fig. 31) was implemented with amplitude equal to 0.25. The results of system simulations are shown in figures 33-37. The system (1) was simulated with the single loop SMC (110), (113), (118) implemented in a PWM format (104) for $\theta_{Lc} = 0.2sign(\sin t)$. A dither signal (fig. 31) was implemented with amplitude equal to 0.5. The results of simulations are shown in figures 38-42. Tracking the load position command profiles look good with both controllers.

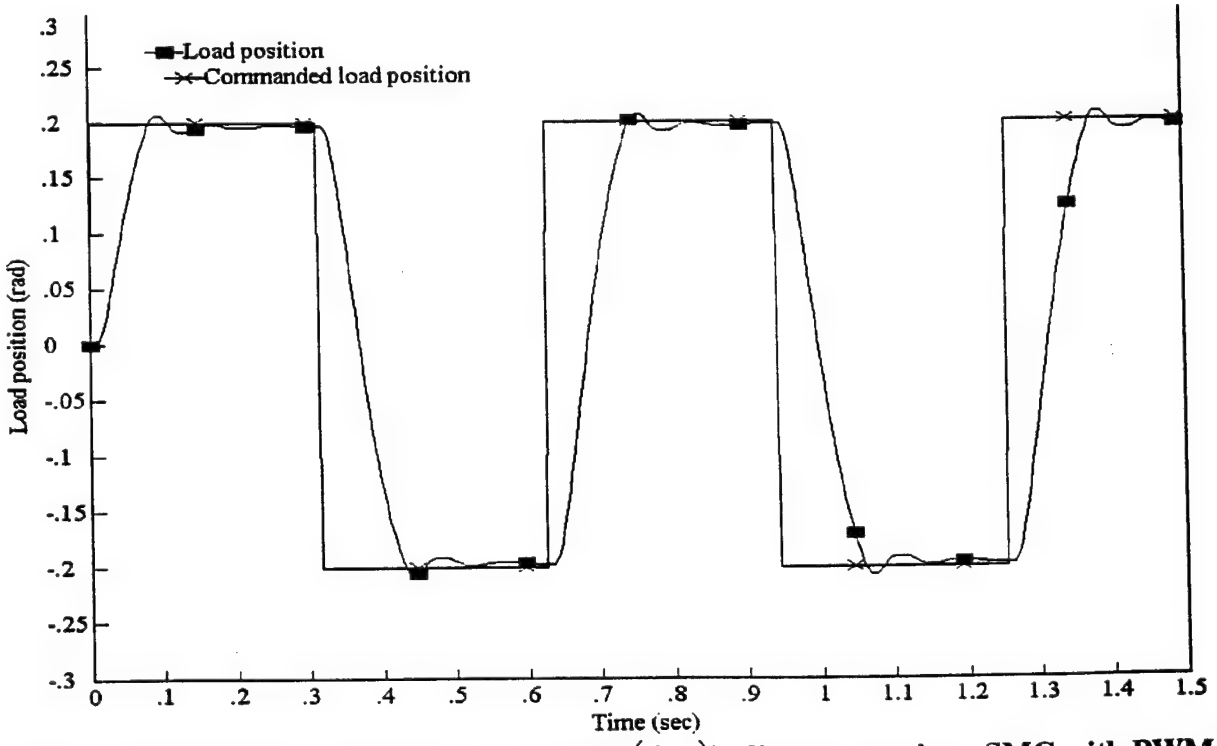

Fig. 33 Load position tracking ($\theta_{Lc} = 0.2sign(\sin t)$), discrete two-loop SMC with PWM

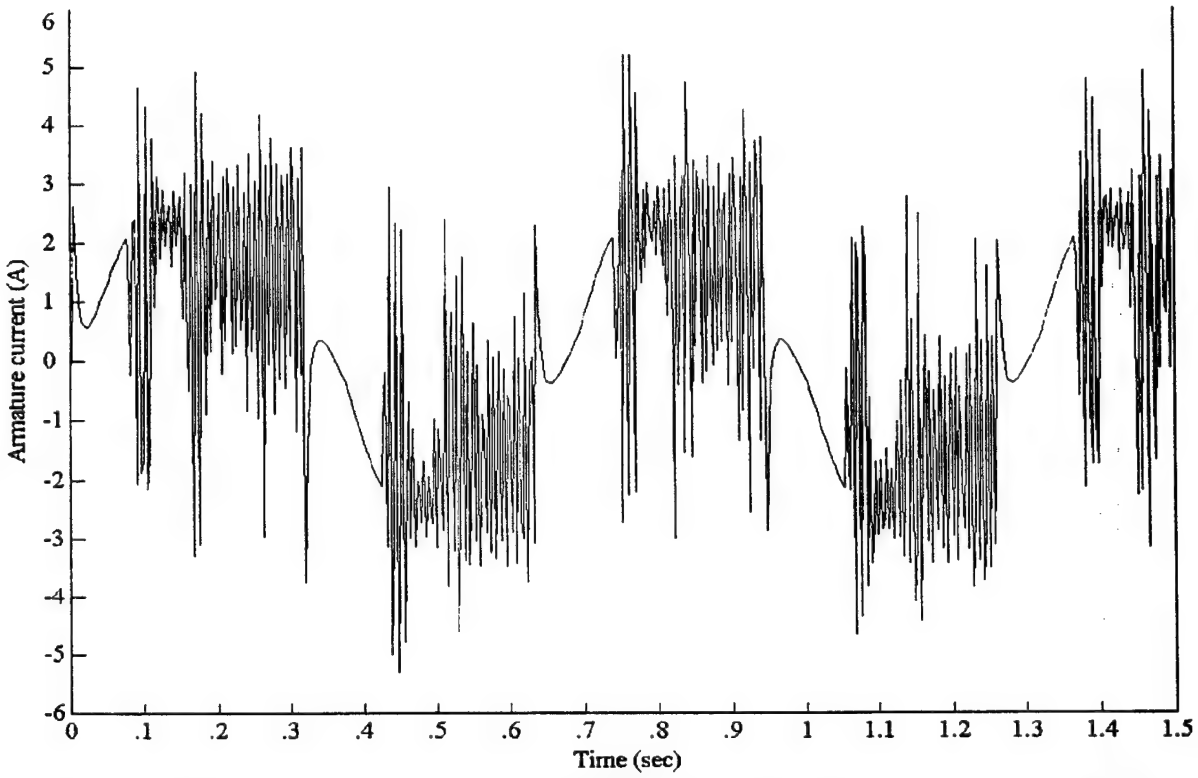

Fig. 34 Armature current ($\theta_{Lc} = 0.2 sign(\sin t)$), discrete two-loop SMC with PWM

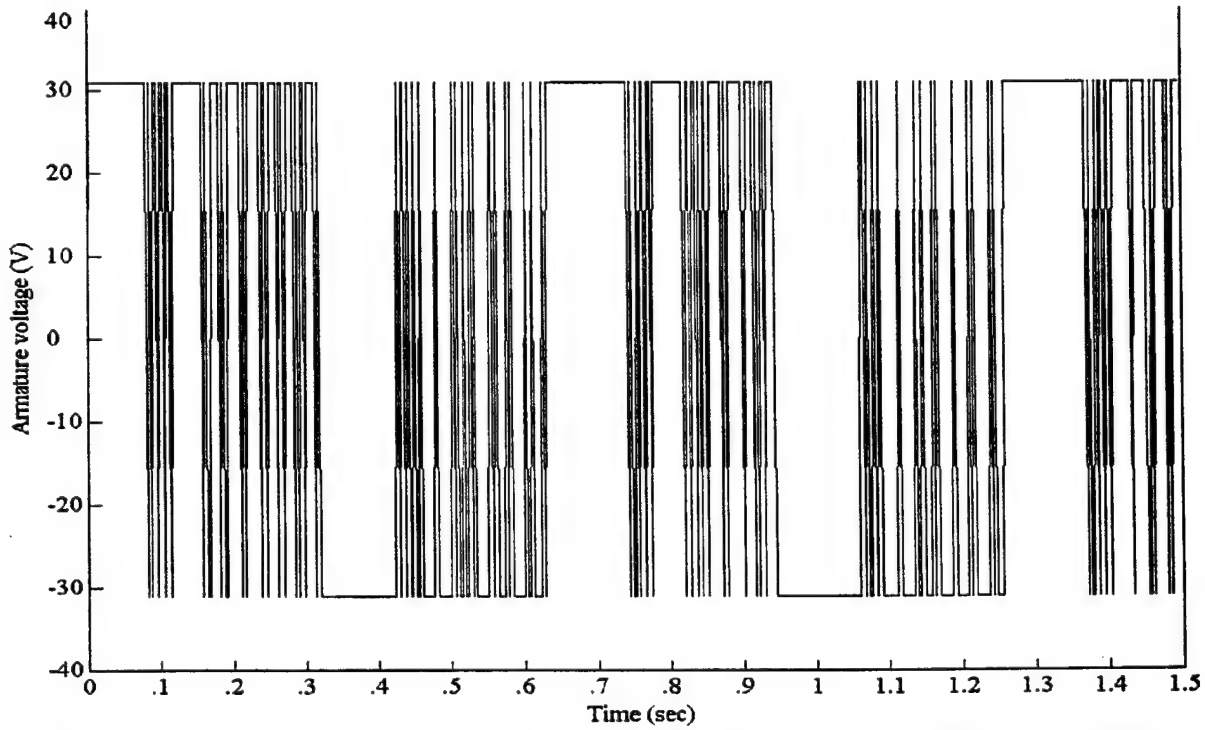

Fig. 35 Armature voltage ($\theta_{Lc} = 0.2 sign(\sin t)$), discrete two-loop SMC with PWM

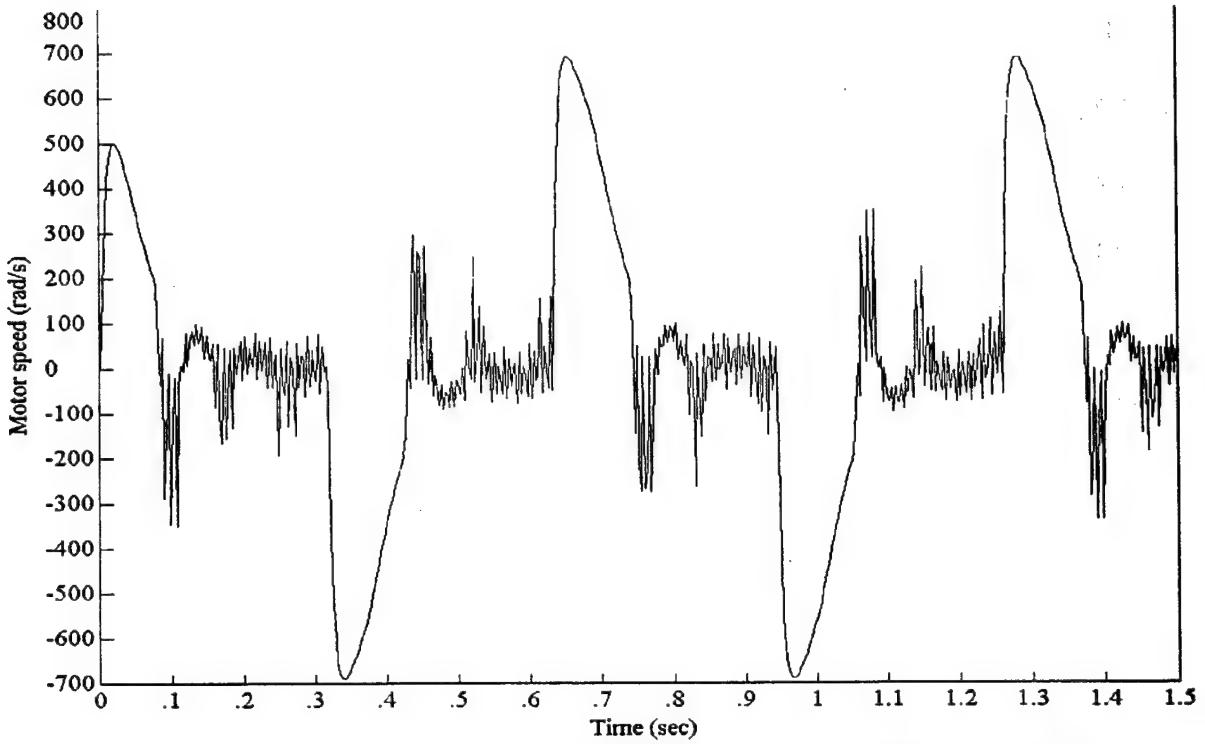

Fig. 36 Motor speed ($\theta_{Lc} = 0.2sign(\sin t)$), discrete two-loop SMC with PWM

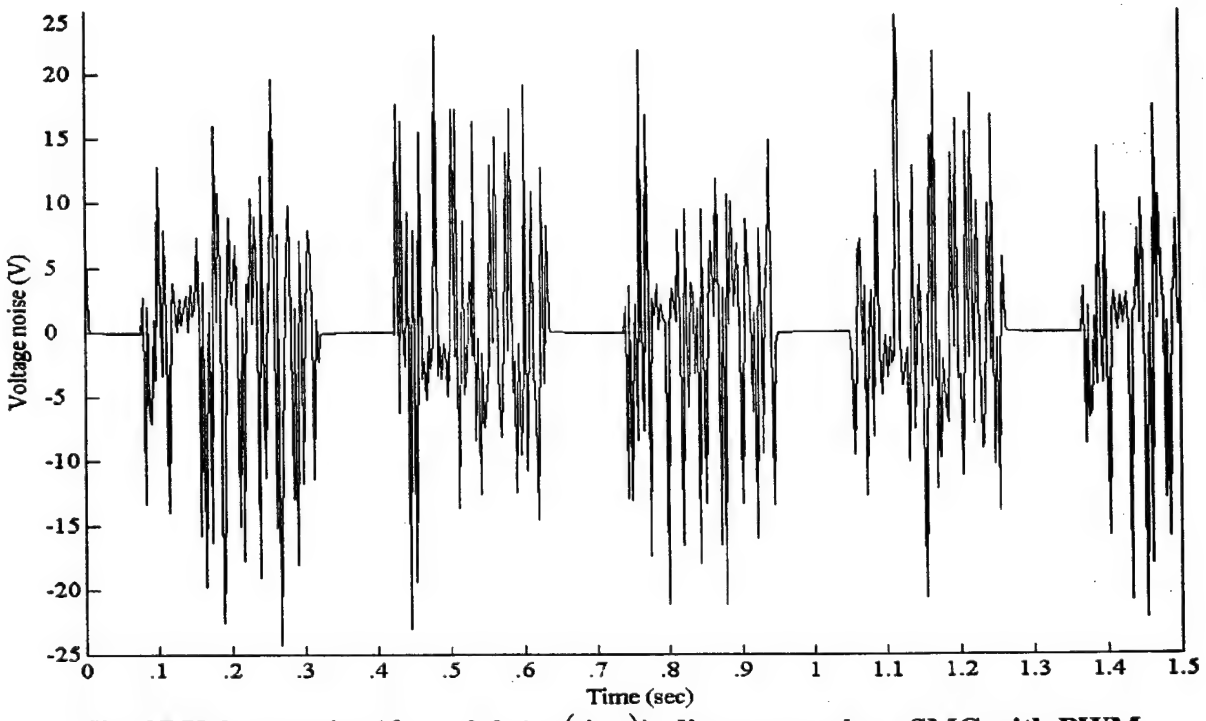

Fig. 37 Voltage noise ($\theta_{Lc} = 0.2sign(\sin t)$), discrete two-loop SMC with PWM

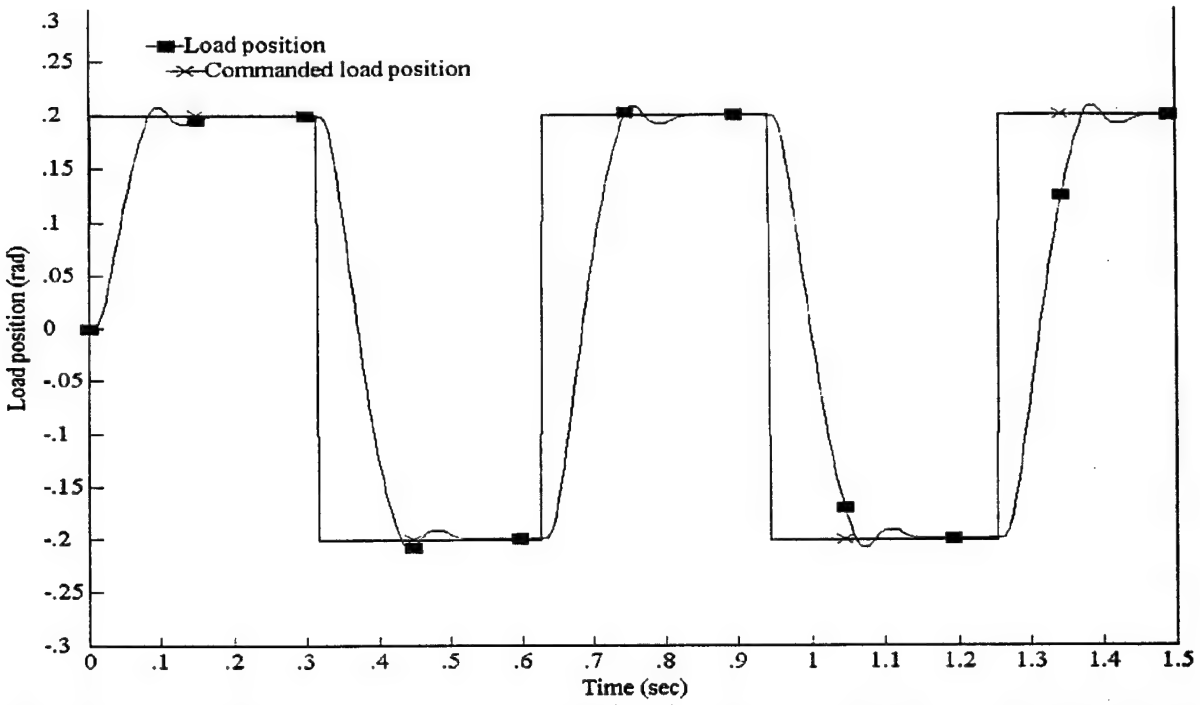

Fig. 38 Load position tracking ($\theta_{Lc} = 0.2 sign(\sin t)$), discrete single-loop SMC with PWM

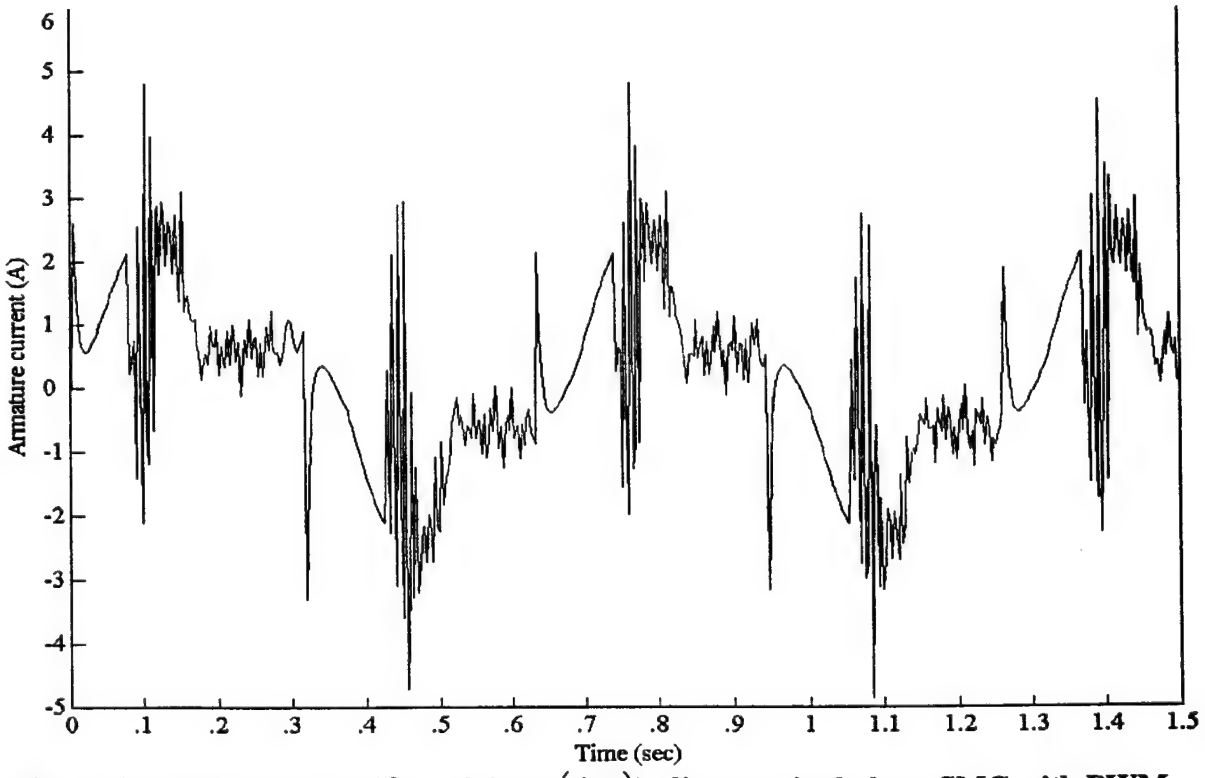

Fig. 39 Armature current ($\theta_{Lc} = 0.2 sign(\sin t)$), discrete single-loop SMC with PWM

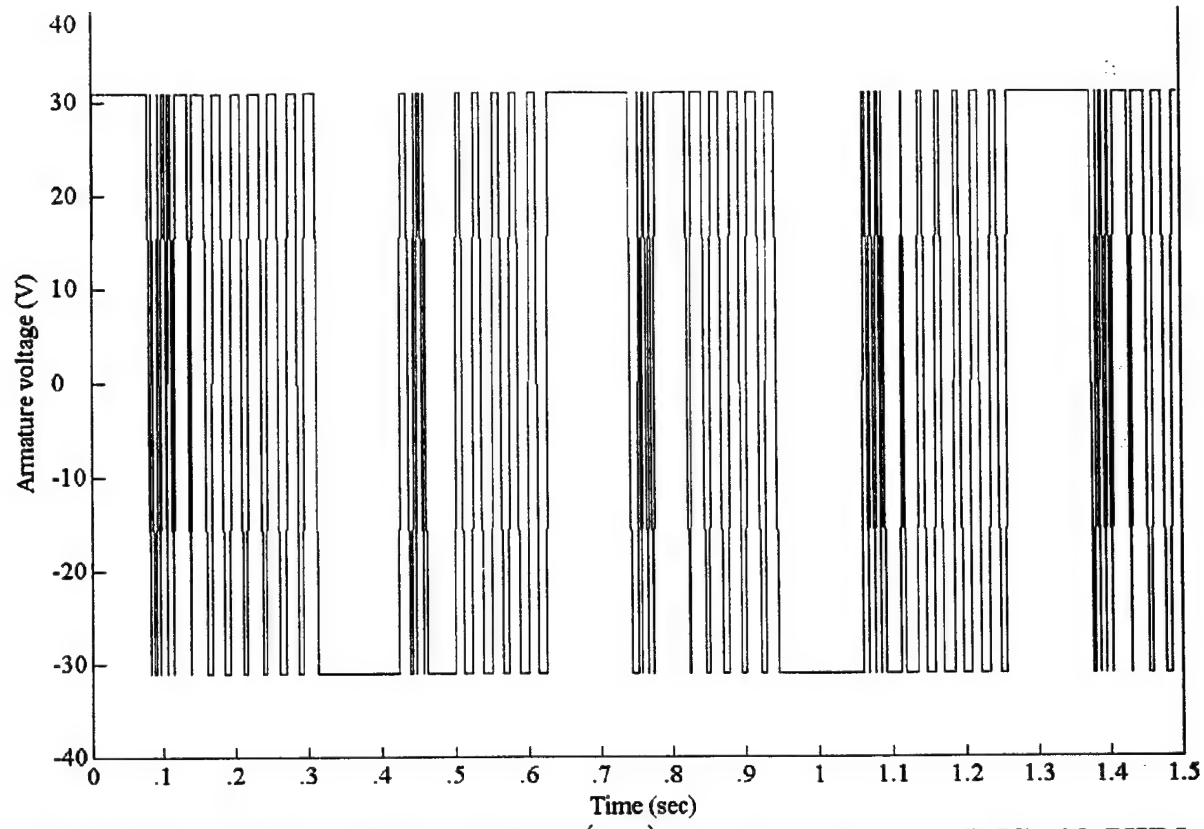

Fig. 40 Armature voltage ($\theta_{Lc} = 0.2sign(\sin t)$), discrete single-loop SMC with PWM

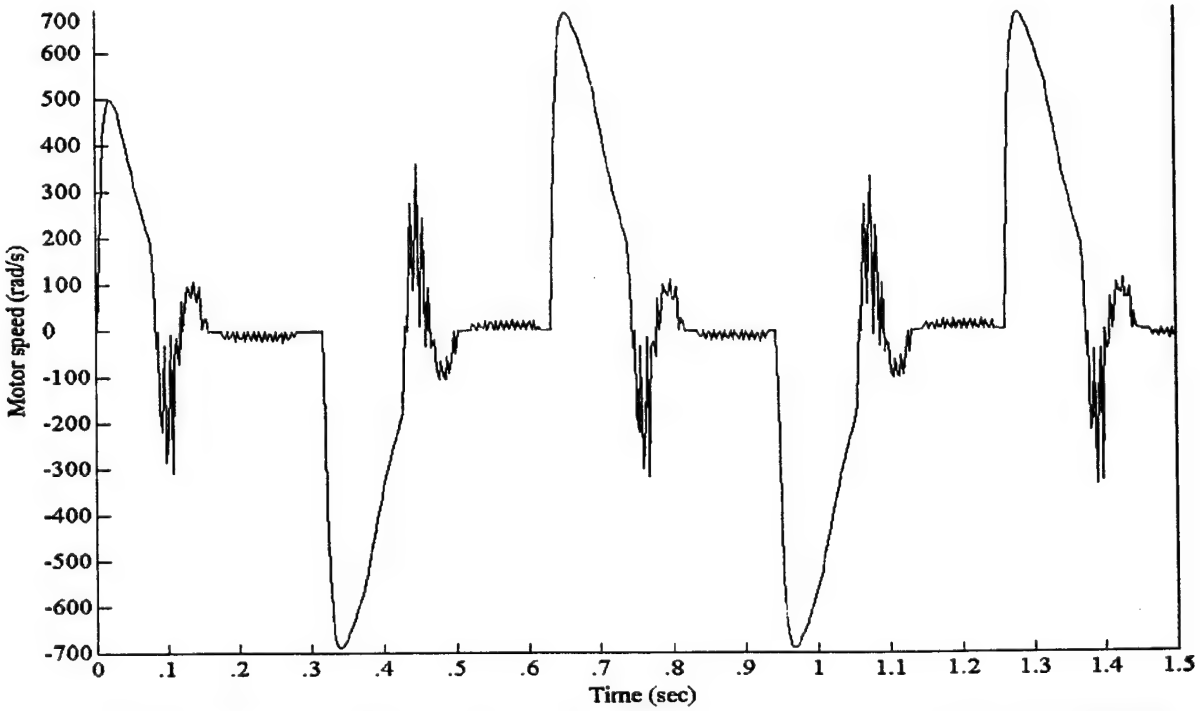

Fig. 41 Motor speed ($\theta_{Lc} = 0.2sign(\sin t)$), discrete single-loop SMC with PWM

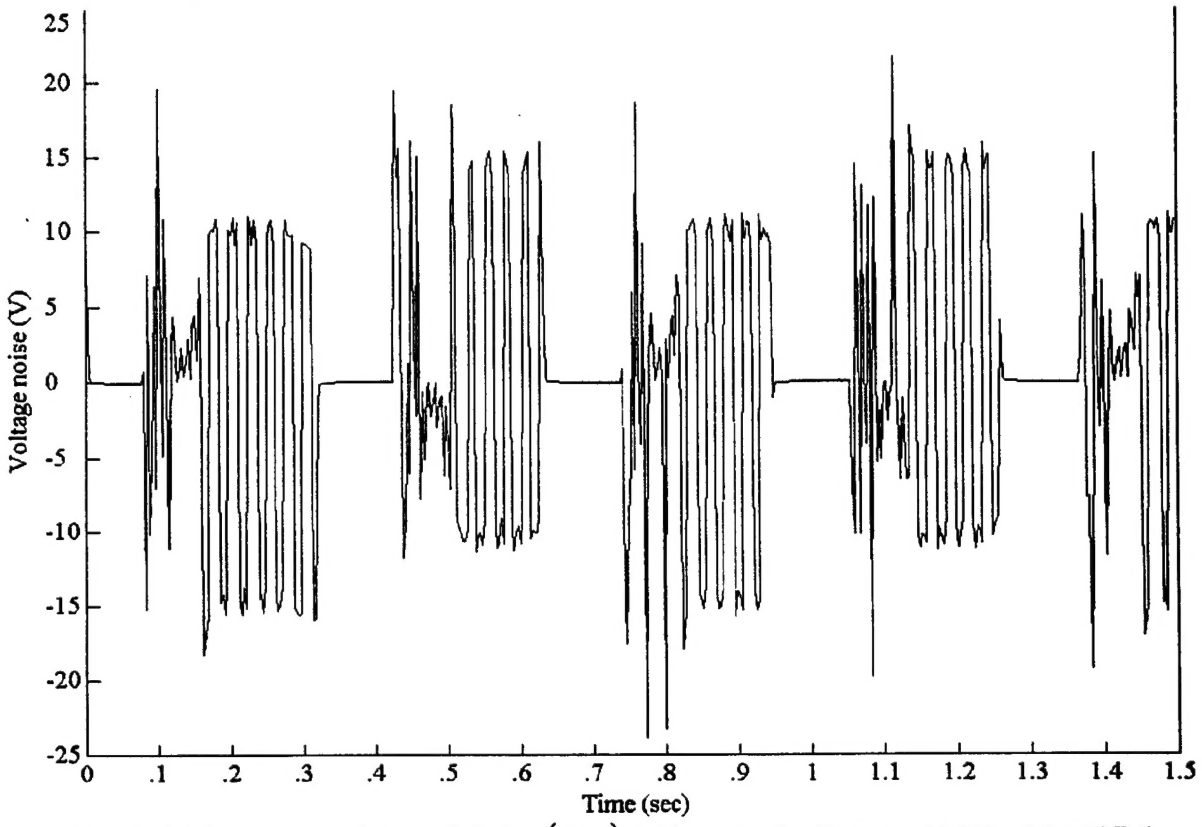

Fig. 42 Voltage noise ($\theta_{Lc} = 0.2 sign(\sin t)$), discrete single-loop SMC with PWM

10. Conclusions

Engineering analysis was performed to investigate the implementation of a sliding mode controller algorithm that will reduce sensitivity to feedback noise in Control Actuation Systems (CAS) such as those used on Guided MLRS, Low Cost Precision Kill (LCPK), and Compact Kinetic Energy Missile (CKEM). The GFE model of the CAS was used to demonstrate performance enhancement achieved with the sliding mode controller for a variety of potential noise sources. Two types of sliding mode controllers: two-loop SMC and single loop SMC were designed addressing the servomechanism output tracking problem. Both SMC demonstrated high accuracy following of load position command profiles. Robustness to disturbances and noise voltage was demonstrated as well. Control voltage operates in a high frequency switching mode

without any special efforts such as PWM. However, simulations of discrete SMC's, that are implemented in a PWM format, showed fewer ripples of armature currents. Also, it is preferable implementing the designed SMC's in the PWM format to protect the controller switching frequency from various noises. Amplitude of a dither signal must be greater then amplitude of summarized noise containing in the sliding surface equation. Implementing the SMC's in the PWM format we can include an integration term in a sliding surface equation to compensate for a possible steady state tracking error.

11. References

[1] Utkin, V. I. *Sliding Modes in Control and Optimization*, Springer-Verlag, Berlin, 1992.

[2] DeCarlo, R. A., Zak, S. H. and Matthews, G. P. "Variable structure control of nonlinear multivariable systems: a tutorial," *IEEE Proceedings,* Vol. 76, pp. 212-232, 1988.

[3] Fernandez, B. R., Hedrick, K. J., Control of multivariable non-linear systems by the sliding mode method, *International Journal of Control,* No. 3., pp. 1019-1040, 1987.

[4] Y. B. Shtessel, "Nonlinear Output Tracking in Conventional and Dynamic Sliding Manifolds," *IEEE Transactions on Automatic Control*, Vol. 42, No. 9, pp. 1282-1286, 1997.

[5] Y. Shtessel, "Decentralized Sliding Mode Control in Three-Axis Inertial Platforms", *AIAA Journal of Guidance, Control and Dynamics*, Vol. 18, No. 4, pp. 773-781, 1995.

[6] Y. Shtessel, "Nonlinear Output Tracking Via Dynamic Sliding Manifolds," *Journal of The Franklin Institute,* Vol. 332B, No. 6, pp. 735-748, 1995.

[7] J. Slotine, Weiping Li, *Applied non Linear Control,* Prentice Hall, Englewood Cliffs, N J, 1991.

[8] F. Esfandiary and H. K. Khalil, "Stability Analysis of a Continuous Implementation of Variable Structure Control," *IEEE Transactions on Automatic Control*, Vol. 36, No. 5, pp. 616-619, 1991.

[9] F. Zhou and D. Fisher, "Continuous Sliding Mode Control," *International Journal of Control*, Vol. 55, No. 2, pp. 313-327, 1992.

[10] Rundell, A. E., Drakunov, S. V., and DeCarlo R. A. "A Sliding Mode Observer and Controller for Stabilization of Rotational Motion of a Vertical Shaft Magnetic Bearing," *IEEE Transactions on Control Systems Technology*, **CSS-4**, No. 5, pp. 598-608, 1996.

[11] M. E. Jackson and Y. B. Shtessel, "Sliding Mode Thermal Control System For Space Station Furnace Facility," *IEEE Transactions on Control System Technology*, Vol. 6, No. 5, pp. 612-622, 1998.

[12] Y. Shtessel, "Sliding Mode Control of the Space Nuclear Reactor System," ***IEEE Transactions on Aerospace and Electronic Systems***, Vol. 34, No. 2, pp. 579-589, 1998.

[13] C. Tournes, B. Landrum, Y. Shtessel and C. Hawk, "Ramjet-Powered Reusable Launch Vehicle Control by Sliding Modes," *AIAA Journal on Guidance, Control, and Dynamics*, Vol. 21, No. 3, pp. 409-415, 1998.

[14] Yuri Shtessel, James McDuffie, Mark Jackson, Charles Hall, Don Krupp, Michael Gallaher, and N. Douglas Hendrix, "Sliding Mode Control of the X33 Vehicle in Launch and Re-entry Modes," *Proceedings of AIAA Guidance, Navigation, and Control Conference*, Boston, MA, August 10-12, paper # AIAA 98-4414, pp. 1352-1362, 1998.

[15] Yuri Shtessel, Jim Buffington, Mayer Pachter, Phil Chandler, and Siva Banda, "Re-configurable Flight Control on Sliding Modes Addressing Actuator Deflection and

Deflection Rate Saturation." *Proceedings of AIAA Guidance, Navigation, and Control Conference,* Boston, MA, August 10-12, paper # AIAA 98-4112, pp. 127-137, 1998.

[16] P. Kokotovic, "The joy of feedback: nonlinear and adaptive." *IEEE Control Systems Magazine,* No. 12, pp. 7-17, 1992.

[17] Y. Shtessel and J. Buffington, "Finite-reaching-time continuous sliding mode controller for MIMO nonlinear systems," *Proceedings of the 37th Conference on Decision and Control,* Tampa, FL, December 16-18, 1998.